The Linnean Society of London ZOOLOGICAL Journal of the Linnean Society

Zoological Journal of the Linnean Society, 2014. With 12 figures

Phylogenetic interrelationships of living and extinct Tinamidae, volant palaeognathous birds from the New World

SARA BERTELLI[1,2]*, LUIS M. CHIAPPE[2] and GERALD MAYR[3]

[1]*Fundación Miguel Lillo-CONICET (Consejo Nacional de Investigaciones Científicas y Técnicas), Miguel Lillo 251, 4000 San Miguel de Tucumán, Argentina*
[2]*The Dinosaur Institute, Natural History Museum of Los Angeles County, 900 Exposition Boulevard, Los Angeles, CA 90007, USA*
[3]*Forschungsinstitut Senckenberg, Sektion Ornithologie, Senckenberganlage 25, D-60325 Frankfurt am Main, Germany*

Received 28 January 2014; revised 10 March 2014; accepted for publication 17 March 2014

Tinamous, one of the earliest diverging living avian lineages, consists of a Neotropical clade of palaeognathous birds with a fossil record limited to the early Miocene–Quaternary of southern South America. Here, we conduct a comprehensive, morphology-based phylogenetic study of the interrelationships among extinct and living species of tinamous. Morphological data of fossil species are included in a matrix of 157 osteological and myological characters of 56 terminal taxa. The monophyly of most recognized genera is supported by the results of the analysis. The cladistic analysis also recovers the traditional subdivision between those tinamous specialized for open areas (Nothurinae) and those inhabiting forested environments (Tinaminae). Temporal calibration of the resultant phylogeny indicates that such a basal divergence had already taken place in the early Miocene, some 17 million years ago. The placement of the fossil species within the open-area (Nothurinae) and the forest-dwelling (Tinaminae) tinamous is also consistent with the palaeoenvironmental conditions inferred from the associated fauna.

doi: 10.1111/zoj.12156

ADDITIONAL KEYWORDS: anatomy – myology – osteology – phylogeny – tinamous.

INTRODUCTION

Tinamous (Tinamidae) include 47 species of Central and South American birds inhabiting forested as well as open environments. Although volant, the flight capabilities of these Neotropical birds are limited (Cabot, 1992). Numerous studies have recognized the monophyly of tinamous and their relationship to the flightless ratites (ostriches, emus, and their relatives), placing both groups within palaeognaths, an early diverging group of modern birds (Cracraft, 1974; Lee, Feinstein & Cracraft, 1997; Livezey & Zusi, 2007; Hackett *et al*., 2008; Harshman *et al*., 2008; Bourdon, Ricqlés & Cubo, 2009; Haddrath & Baker, 2012; Worthy & Scofield, 2012; Smith, Braun & Kimball, 2013).

Regarding habitat preferences, Miranda-Ribeiro (1937) proposed two general categories of tinamous, and grouped the known genera into two subfamilies: one harbouring the forest tinamous, Tinaminae (*Tinamus*, *Crypturellus*, and *Nothocercus*), and the other composed of open-area or aridland tinamous, Nothurinae (*Taoniscus*, *Nothura*, *Nothoprocta*, *Rhynchotus*, *Eudromia*, and *Tinamotis*). However, with the exception of Miranda-Ribeiro's and a few other early studies of external morphology (Salvadori, 1895; von Boetticher, 1934), the relationships between the many species of tinamous remained poorly studied until recently (Bertelli, 2002; Bertelli, Giannini & Goloboff, 2002; Porzecanski, 2003; Bertelli & Chiappe, 2005; Bertelli & Giannini, 2013). The first modern comprehensive

*Corresponding author. E-mail: sbertelli@lillo.org.ar

study of the phylogenetic interrelationships of tinamous was conducted by Bertelli *et al*. (2002), who produced a hypothesis supporting the monophyly of Nothurinae but highlighting paraphyly of Tinaminae. This analysis was based on external morphological characters (and was recently re-evaluated by Bertelli & Giannini, 2013). Similar results were obtained by a less inclusive osteological analysis (Bertelli & Chiappe, 2005), but the molecular-based study of Porzecanski (2003) supported the monophyly of both Tinaminae and Nothurinae.

Tinamous have a scant South American fossil record represented by fragmentary remains spanning the last 17 million years (Tonni, 1977; Tambussi & Tonni, 1985; Tambussi, 1987, 1989; Chiappe, 1991; Tambussi, Noriega & Tonni, 1993; Tambussi & Noriega, 1996; Bertelli & Chiappe, 2005). All Cenozoic records are limited to Argentina; only Pleistocene remains are known from outside of Argentina, in Peru and Brazil (Brodkorb, 1963; Campbell, 1979). The oldest known fossils of this group are early Miocene tinamous from the Pinturas and Santa Cruz formations of southern Patagonia (Argentina), including the extinct species *Crypturellus reai* Chandler, 2012 (Chiappe, 1991; Bertelli & Chiappe, 2005; Chandler, 2012). A late Miocene (Epecuén Formation) tinamou from La Pampa Province in Argentina was described as an indeterminate species of *Eudromia* (Tambussi, 1987), and two extinct species, *Eudromia olsoni* Tambussi & Tonni, 1985 and *Nothura parvula* Tambussi, 1989, were based on fossils found in sediments from the Pliocene of Buenos Aires Province (Monte Hermoso and Chapadmalal Formations), also in Argentina. Although Tertiary records appear to belong to extinct taxa, most Quaternary tinamous have been assigned to living species. The published exceptions are *Nothura paludosa* Mercerat, 1897 and an unnamed species of *Nothura*, both from the Pleistocene of Argentina (Mercerat, 1897; Picasso & Degrange, 2009).

Here we review the interrelationships of Tinamidae based on osteological and myological characters, including known fossil representatives of this clade. The distribution of the fossil tinamous within the resultant cladograms is discussed in light of their significance for understanding the evolution of the two main ecological subdivisions of these birds: the forest-dwelling taxa, traditionally classified in the taxon Tinaminae, and the open-area tinamous (Nothurinae).

MATERIAL AND METHODS

Taxon sampling

Out-group comparisons were made with members of Palaeognathae [*Apteryx australis* (Shaw and Nodder, 1813), *Rhea americana* (Linnaeus, 1758), and the fossil *Lithornis*], and codings from two species of *Lithornis* (*Lithornis celetius* Houde, 1988 and *Lithornis vulturinus* Owen, 1840) were combined to form a single supraspecific terminal (*Lithornis*) representing Lithornithidae. Additionally, galliform [*Leipoa ocellata* Gould, 1840, *Penelope superciliaris* Temminck, 1815, and *Coturnix coturnix* (Linnaeus, 1758)] and anseriform taxa (*Chauna torquata* Oken, 1816, *Mergus serrator* Linnaeus, 1758, and *Anas flavirostris* Vieillot, 1816) were added to the taxonomic sample, as these birds are widely accepted as early divergences of Neognathae (e.g. Ericson *et al*., 2006; Livezey & Zusi, 2007; Hackett *et al*., 2008). The root was placed on the Mesozoic non-neornithine bird *Ichthyornis dispar* Marsh, 1872 (Clarke, 2004).

The in-group included 37 extant taxa (from all tinamou genera) that could be scored unambiguously in the context of our studied characters: 37 currently recognized species, with *Rhynchotus maculicollis* (Gray, 1867) treated as a separate species, following Maijer (1996). To test the phylogenetic affinities of the fossil tinamous, we scored the morphological information of the extinct representatives of Tinamidae (nine fossil taxa; Table 1). Although it is not possible to ascertain the number of species of the oldest fossil remains (Bertelli & Chiappe, 2005), we scored these unnamed tinamous as four different terminals based on differences between the character states scored for the fossils (see Table 1). No differences between scorings for both MACN-SC-1440 and MACN-SC-1399 (the tibiotarsi), and MACN-SC-360 and MACN-SC-1449 (humeri), were found; therefore, these specimens were treated as terminal units, respectively, and scored as MACN-SC-T and MACN-SC-H in the data matrix (Appendix 1). Coracoids MACN-SC-3610 and MACNSC-3613 were scored differently and were treated as separate terminals. Because the other coracoids (MACN-SC-3609, MACN-SC-3611, and MACN-SC-3612) could not be differentiated from either MACN-SC-3610 or MACN-SC-3613, they were not treated as separate terminal units (Bertelli & Chiappe, 2005).

The extinct species *Crypturellus reai* Chandler, 2012, *Eudromia olsoni* Tambussi and Tonni, 1985, *Nothura parvula* Tambussi, 1989, and the indeterminate species of *Nothura* (Picasso & Degrange, 2009) and *Eudromia* (Tambussi, 1987) were also included in the cladistic analysis (Table 1). There is no available information (holotype possibly lost) on the Pleistocene *Nothura paludosa* Mercerat, 1897, and for this reason the species could not be incorporated in the present study. Finally, fossils considered conspecific with the living species of Tinamidae were not included (assuming the identifications of Quaternary fossils assigned to extant species of tinamous are correct).

Table 1. Fossil tinamous

Source	Material	Taxonomy	Horizon	Locality
MACN-SC-1399	Tibiotarsus (distal end)		Pinturas Formation, early–middle Miocene	Portezuelo Sumich, Santa Cruz Province, Argentina
MACN-SC-3610	Coracoid (proximal end)			
MACN-SC-3613	Coracoid (proximal end and shaft)			
MACN-SC-3609	Coracoid (nearly complete)			
MACN-SC-3611	Coracoid (proximal end and shaft)		Santa Cruz Formation, early–middle Miocene	Monte Observación, Santa Cruz Province, Argentina
MACN-SC-3612	Coracoid (proximal end and shaft)	Tinamidae (after Bertelli & Chiappe, 2005)		
MACN-SC-1449	Humerus (distal end)			
MACN-SC-1440	Tibiotarsus (distal end)			Monte León, Santa Cruz Province, Argentina
MACN-SC-360	Humerus (distal end)			Cañadón de las Vacas, Santa Cruz Province, Argentina
AMNH FAM 9151	Humerus (complete)	*Crypturellus reai* Chandler, 2012		
MLP 87-XI-20-3	Coracoid (nearly complete)	*Eudromia* sp. Tambussi, 1987	Epecuén Formation, late Miocene	Salinas Grandes, La Pampa Province, Argentina
MACN-16597	Humerus (proximal end, shaft), femur (distal end), pelvis (incomplete), tibiotarsus	*Eudromia olsoni* Tambussi and Tonni, 1985		
MACN-16596	Humerus, carpometacarpus, radius, scapula (cranial end), coracoid (nearly complete), ulnae (shaft and distal end), femur (shaft and proximal end), tarsometatarsus		Monte Hermoso Formation, early–middle Pliocene	Barrancas del Litoral Atlántico, 17 km south-west of Pehuén-Co, Buenos Aires Province, Argentina
MLP-34-V-10-9	Humerus			Baliza chica, Miramar, Buenos Aires Province, Argentina
MLP-68-XII-3-1	Tibiotarsus (distal end), tarsometatarsus, femur (proximal end), phalanges	*Nothura parvula* Tambussi, 1987	Chapadmalal Formation, middle–late Pliocene	Río Quequén Salado, Buenos Aires Province, Argentina
MLP-63-VII-30-1	Coracoid	*Eudromia* cf. *olsoni* Tambussi, 1987		
MLP-52-X-5–33	Coracoid			Miramar, Buenos Aires Province, Argentina
Picasso & Degrange (2009)	Coracoid	*Nothura* sp.*	Ensenada Formation, early–middle Pleistocene	Punta Indio, north-east of Buenos Aires Province, Argentina
MLP?	Femur	*Nothura paludosa*** Mercerat, 1897	Buenos Aires Formation, late Pleistocene	Arrecifes, Buenos Aires Province, Argentina

*Specimens of the taxa listed have been observed directly (except for *Nothura* sp., taken from the respective bibliographic references).
**No available information of this specimen (missing from the Museo de La Plata Palaeontological Collection).

Characters

The morphological data set of this study included 157 anatomical characters (117 osteological and 40 myological characters; see Appendix 2). All osteological character codings for extant and fossil taxa were re-examined by direct study of skeletal material (except for *Nothura* sp., see Table 1). The present study builds upon the osteological analysis of Bertelli & Chiappe (2005). We further expanded, rescored, or modified this information (mainly because of problems in the definition of character states, see comments on Appendix 2), added more characters (as well as in-group and out-group taxa), and incorporated myological information from the literature (see below). To corroborate the identification of osteological structures or coding, we also reviewed the anatomical descriptions provided by Parker (1866), Lucas (1886), Pycraft (1900), Verheyen (1960), and Saiff (1988). Finally, we also incorporated some characters that clarify the phylogenetic relationships of Palaeognathae and basal Neognathae, which were described and discussed previously by other authors (see comments on character descriptions in Appendix 2). In total, we scored 117 osteological characters that included absence and presence, relative development, and relationships of cranial and postcranial bony structures of the fossil and living tinamous and out-group terminals (Figs 3–12). All of the character states were scored from museum specimens (Appendix S1). For the myological characters, we based our scoring on comprehensive descriptions of the cranial and appendicular musculature of tinamous (Hudson *et al.*, 1972; Elzanowski, 1987), which included representatives of 19 species of our in-group terminals. We also reviewed detailed anatomical studies provided by Alix (1874) on *Tinamus major* (Gmelin, 1789) (= *Nothura major* of Alix, 1874), by Lakjer (1926) on *Crypturellus obsoletus* (Temminck, 1815), and by Dzerzhinskii (1983) on the cranial myology of *Eudromia elegans* (Saint-Hilaire, 1832). We have excluded from the analysis characters that are non-informative (owing to the presence of a condition in only one terminal taxon), despite the fact that future myological studies could possibly demonstrate that these characters are phylogenetically informative. We coded distinct descriptive statements for each recognized structure, such as presence and absence, divisions and fusions, and variations in origin and attachment of muscles and tendons, constraining the use of myological information to cases in which the morphological variation described could be distinctly scored in discrete character states. This resulted in 40 myological characters; the total morphological matrix of 157 characters of the internal anatomy is provided in Appendix 2. Descriptions and morphological comparisons follow the nomenclature of Baumel *et al.* (1993).

Cladistic analysis

The phylogenetic analysis was conducted using equally and weighted parsimony in TNT 1.0 (Goloboff, Farris & Nixon, 2008a, 2008b). All analyses included 1000 replicates of Wagner trees (using random addition sequences), followed by tree bisection reconnection (TBR) branch swapping, keeping up to ten trees per replication. The best trees obtained at the end of the replicates were subjected to a final round of TBR branch swapping. Zero-length branches were collapsed if they lacked support under any of the most parsimonious reconstructions. To estimate the support of groups, we report results from a jackknife resampling of characters using GC frequencies in 1000 replicates of symmetric resampling ($K = 3$), as described by Goloboff *et al.* (2003), to examine the most-parsimonious trees (MPTs) in which the monophyly of a given group is rejected (Fig. 1). To improve the tree resolution, unstable taxa were identified over the entire set of MPTs (Pol and Escapa, 2009). The oldest, fragmentary, tinamou remains MACN-SC-T and MACN-SC-H (see Taxon sampling), the extinct species *Crypturellus reai*, and *Nothura* sp. (Table 1) were pruned from the MPTs (a posteriori of the heuristic tree searches) to construct a reduced strict consensus, provide diagnosis of some relevant clades that collapsed in the complete strict consensus, and evaluate nodal support (Fig. 1).

RESULTS

Interrelationships of extant taxa

Tree searches under equal weights resulted in 23 MPTs of 454 steps found in 998 of the 1000 replicates. The additional TBR round on those trees did not yield other optimal trees. Analysis under implied weights recovered five trees in 770 of the 1000 replicates (45.177 weighted steps). The strict consensus tree was largely resolved, with nearly identical topologies under analyses with equal and implied weight (see strict consensus in Fig. 1). Out-group relationships were mostly resolved and well supported (Fig. 1), with the exception of the position of *Lithonis* sp. (although note that we did not include characters to specifically resolve the placement of this taxon). The in-group subtree was broadly resolved (see strict consensus in Fig. 1). Only some groups with low stability (i.e. relationships within *Crypturellus*) varied across these analyses. Levels of branch stability were concordant across equal and implied weight analyses, best-supported clades on absolute terms also showed little conflict (high relative support values; Fig. 1). In the consensus topology, a monophyletic Tinamidae is recovered with high support (GC 100; Fig. 1). The analysis identified 13 osteological synapomorphies for Tinamidae: dorsal position of foramen v. occipitalis externa relative to the prominentia

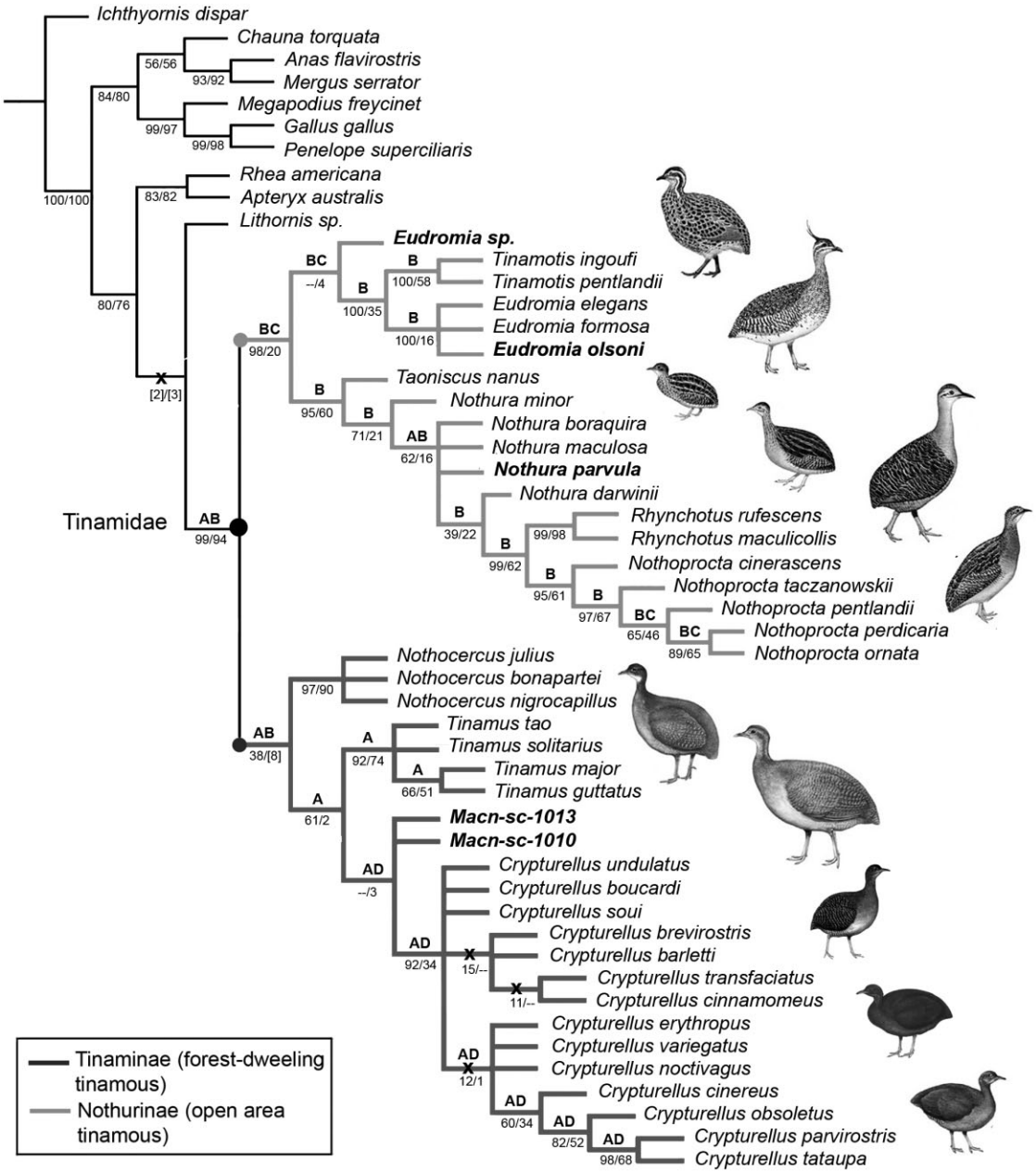

Figure 1. Reduced strict consensus of the phylogenetic analysis of fossils and living tinamous under implied weight. Differences between topologies under equal versus implied weights analyses are marked with an '×'. Alternative positions of the fossils excluded from the strict consensus a posteriori are indicated above branches (A, MACN-SC-H; B, MACN-SC-T; C, *Nothura* sp.; D, *Crypturellus reai*). Support values of the phylogenetic analysis of extant species and analysis including fossils, respectively, are below branches.

cerebellaris (character 0, Fig. 3E–H), foramen n. vagi widely separated from foramen n. ophthalmici (character 4, Figs 3E, F, and 5A–D), slightly decurved ramus mandibularis (character 39, Fig. 4A, B, D, E), notarium with four fused vertebrae (character 57, Fig. 7J), sternum with laterally projected processus craniolateralis (character 58, Fig. 8A, B), spina interna of sternum present (character 60, Fig. 8A–H), a well-developed dorsal foramen below cotyla scapularis of coracoid (character 69, Fig. 9O, P), shallow facies articularis scapularis of coracoid (character 74, Fig. 9O, P), ventral condyle of humerus longer than dorsalcondyle (character 83, Fig. 9G, H), praeacetabular region distinctly longer than caudal portion of ilium (character 92, Fig. 10D–F, H,

I), well-developed tuberculum praeacetabulare (character 99, Fig. 10E, F, H), somewhat projected crista trochanteris of femur (character 100, Fig. 11C), and the presence of a pons supratendineus of the tibiotarsus (character 107, Fig. 11G–L).

Based on the present analysis, Tinamidae is subdivided into two groups: the forest-dwelling Tinaminae (*Crypturellus*, *Tinamu*s, *Nothocercus*) and open-area Nothurinae (*Taoniscus*, *Nothura*, *Nothoprocta*, *Eudromia*, *Tinamotis*, and *Rhynchotus*; Figs 1 and 2). With the exception of *Nothura*, almost all currently recognized polytypic genus-level taxa of tinamous were recovered with high support (GC > 91; Fig. 1).

The Tinaminae is diagnosed by seven osteological apomorphies: an incomplete row of supraorbital ossicles (character 12, Fig. 3C), a wide sulcus and foramen n. olfactorii (character 15, Fig. 4B, D), a mediolaterally wide processus maxillares and maxillopalatini (character 32, Fig. 5B), a mandibula with converging grooves of the ventral surface (character 36), a distinct facies articularis parasphenoidalis (character 43, Fig. 6B), a rounded processus supracondylaris dorsalis of the humerus (character 85, Fig. 9G, H), a tibiotarsus with a long condylus lateralis (character 104, Fig. 11H, I, K, L), and a nearly enclosed canal for m. flexor digitorum longus (character 111, Fig. 12G). The osteological evidence supporting the clade also brings a considerable measure of conflict (GC 24; Fig. 1). When Tinaminae is not recovered as a monophyletic group, the resultant topologies are moderately suboptimal, implying four extra steps when it is depicted as non-monophyletic.

Trees depicting Nothurinae as non-monophyletic require more than eight extra steps and, therefore, the osteological and myological information strongly supports the open area clade (GC 97; Fig. 1). The skull of Nothurinae is characterized by a small temporal notch (character 5, Fig. 4A, C, E), with a wide incisura for ductus lacrimalis (character 21, Fig. 4A, E), and the quadratum possesses a conspicuous prominentia submeatica (character 47, Fig. 6H–J). Postcranially, open-area tinamous are characterized by a coracoid with a distinct procoracoideal crest (character 75, Fig. 9P), a hook-shaped crista bicipitalis of the humerus (character 80, Fig. 9A, F), and tarsometatarsus significantly shorter than femur (character 101), with a single hypotarsal ridge (character 110, Fig. 12F, H). In addition, five myological characters are unambiguous apomorphies of this clade: the ligamentum postorbitale originates from the frontal part of the processus postorbitalis (character 118), the aponeurosis parabasalis attaches to both the postmeatic area and lamina basitemporalis (character 124), the pars caudalis of the m. adductor mandibulae externus is absent (character 125), the pars profunda and superficialis of the m. adductor mandibulae externus are partially fused (character 128), and the m. protractor pterygoidei et quadrati is bipartite (character 138).

Within the forest-dwelling tinamous, *Nothocercus* (GC 99; Fig. 1) is the earliest diverging taxon of Tinaminae, and the relationships within this clade are unresolved. The monophyly of this genus was supported by the following osteological synapomorphies: a mandible with a weakly developed processus parasphenoidalis medialis (character 24), and a medial crest marked on lamina parasphenoidalis (character 25), a poorly developed processus lateralis of coracoid (character 76, Fig. 9S), a processus flaxorius of the humerus that projects beyond the ventral condyle (character 87, Fig. 9G), the cranial end of the ilium being rounded and markedly expanded laterally (character 94, Fig. 10I, J), and a deeply excavated fossa parahypotarsalis lateralis of tarsometatarsus (character 113, Fig. 12C).

Next, *Tinamus* and *Crypturellus* are grouped together with high support (GC 8; Fig. 1), and share the presence of glandular depressions (character 11, Fig. 3A) and a paired, complete row of ossicula supraorbitales (character 12, Fig. 3A) on the skull, a sternum with poorly projected processus craniolateralis (character 58, Fig. 8H), an expanded scapular blade (character 68, Fig. 8L), a coracoid with an overhanging tuberculum brachiale (character 70, Fig. 9Q), and a groove for the origin of ligamentum acrocoracohumerale contacting the facies articularis clavicularis (character 71, Fig. 9P).

A monophyletic *Tinamus* (GC 96; Fig. 1) is supported by the following ostcranial characters: synsacrum with a flat centrum and wide processus costales (character 54), spina interna rostri markedly elongate (character 62, Fig. 8H), ulna distinctly longer than humerus (character 88), preacetabular and postacetabular portions of pelvis of subequal length (character 92; Fig. 10C, G), markedly projected crista trochanteris of femur (character 100, Fig. 11D), tarsometatarsus about the same length as the femur (character 101), and condylus lateralis with angular proximal margin, widening distally (108, Fig. 11E). *Tinamus major* + *Tinamus guttatus* (Pelzeln, 1863) form a relatively well supported clade (GC 59; Fig 1), characterized by a notarium with three fused vertebrae (character 53, Fig. 7I) and a deep fossa parahypotarsalis lateralis of the tarsometatarsus (character 113; Fig. 12C).

Crypturellus is recovered with good support (GC 91; Fig. 1). Its monophyly is supported by cranial, postcranial, and myiological apomorphies: a narrow interorbital area (character 13, Fig. 3A), a curved processus orbitalis of the quadrate, flaring out at tip (character 48, Fig. 6H, K), the spina interna rostri of the sternum being narrower than the craniolateral process (character 61, Fig. 8E), a coracoid with a flat processus acrocoracoideus (character 72, Fig. 9T), the proximal margin of the cotyla scapularis with

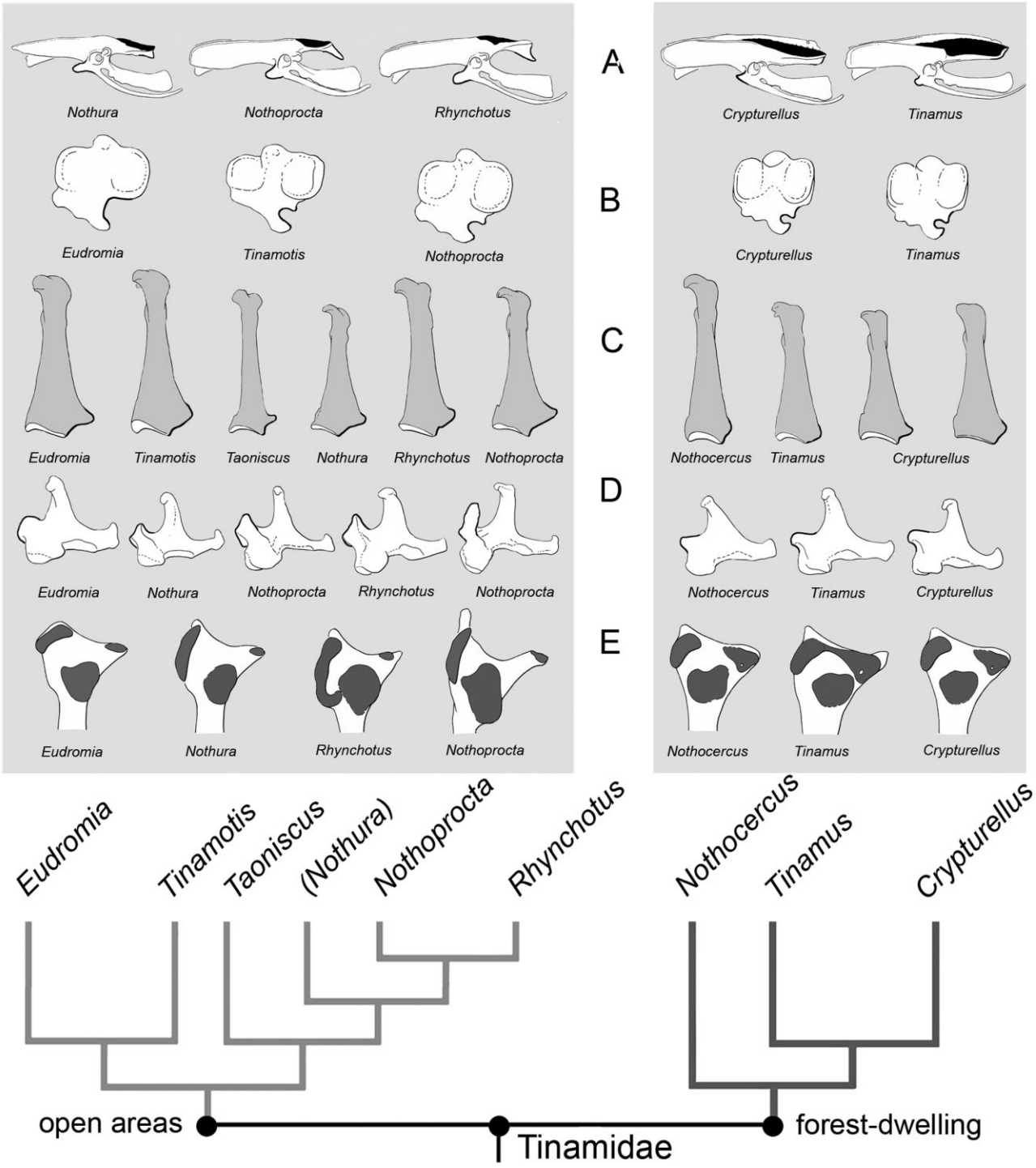

Figure 2. Osteological characters supporting tinamou relationships. A, pelvis, relative length of cranial and caudal portions of ilium (character 92), extension of caudal end (character 97), and development of the tuberculum praeacetabulare (character 99); B, tarsometatarsus, opening of hypotarsal sulcus/canal for m. flexor digitorum longus (character 111); C, coracoid, development of processus lateralis (character 76); D, quadratum, projection of prominentia submeatica (character 47); E, shape of cotylae mandibulares (characters 42–44). The numbers denote characters and character states as described in in Appendix 2. Figures not drawn to scale.

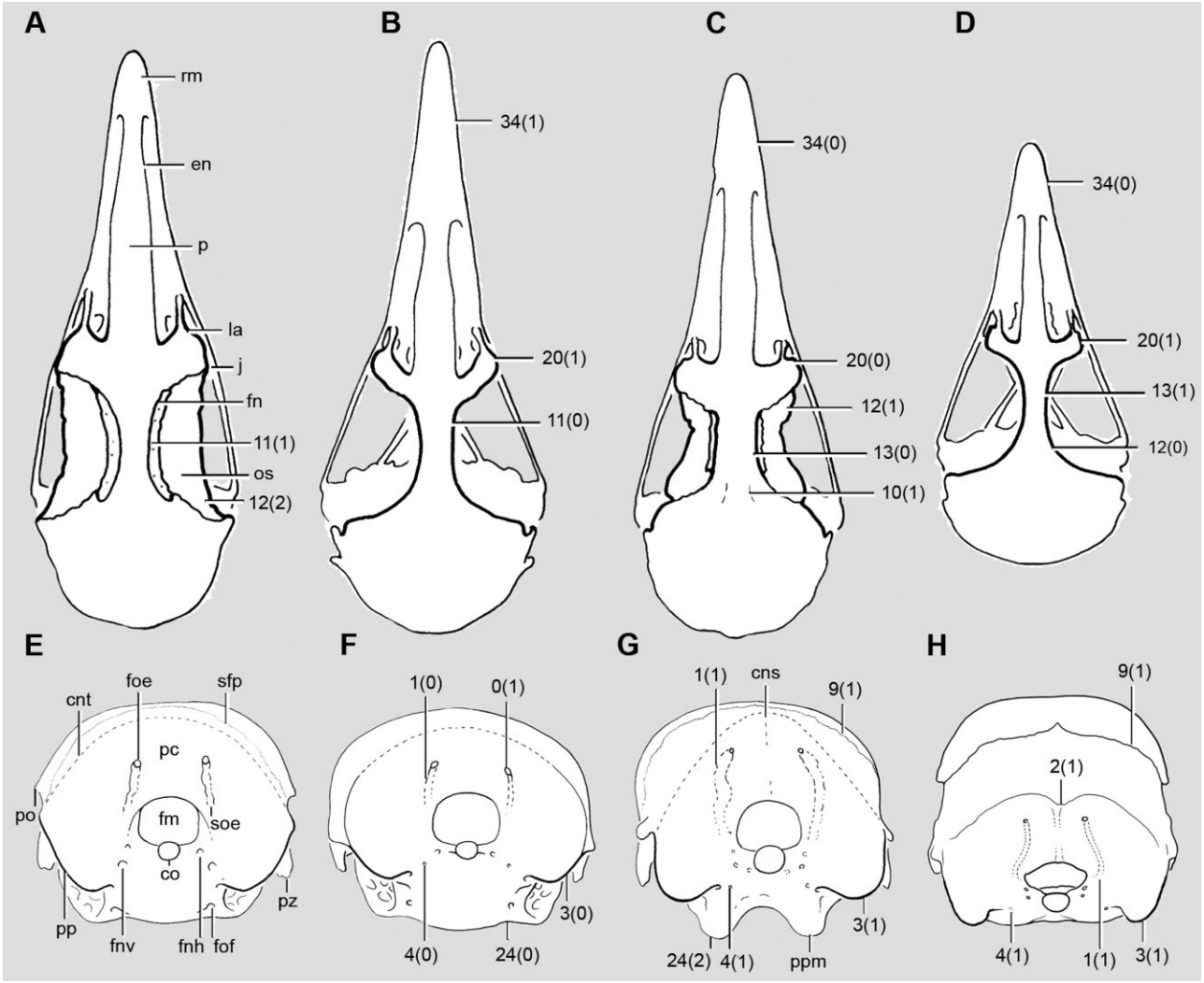

Figure 3. A–D, skulls in dorsal view: *Crypturellus undulatus* (A); *Nothoprocta ornata* (B); *Eudromia formosa* (C); and *Nothura maculosa* (D). E–H, skulls in occipital view: *Crypturellus cinnamomeus* (E); *Taoniscus nanus* (F); *Nothoprocta taczanowskii* (G); and *Rhynchotus maculicollis* (H). Abbreviations: cns, crista nuchalis sagittalis; cnt, crista nuchalis transversa; co, condylus occipitalis; en, external nares; fm, foramen magnum; fn, fossa glandulare nasalis; fnh, foramen n. hypoglossi; fnv, foramen n. vagi; foe, foramen v. occipitalis externa; fof, foramen n. ophthalmici; j, os jugale; la, os lacrimale; os, ossicula supraorbitales; p, pila supranasalis; pc, prominentia cerebellaris; po, processus postorbitalis; pp, processus paroccipitalis; ppm, processus parasphenoidalis medialis; pz, processus zygomaticus; rm, rostrum maxillare; sfp, sutura frontoparietalis; soe, sulcus v. occipitalis externa. The numbers denote characters and character states as listed in Appendix 2. Figures are not drawn to scale.

pneumatic openings (character 73, Fig. 9P), a distinctly projected crest at the base of the processus procoracoideus (character 75, Fig. 9P), a humerus with an incisura capitis obstructed by a tubercle (character 79, Fig. 9F), and a crista bicipitalis with a hook-shaped extension (character 80, Fig. 9F), the tarsometatarsus being shorter than the femur (character 101), a bipartite insertion of the ligamentum jugomandibulare externum (character 120), a bipartite ligamentum quadratomandibulare rostrale (character 122), the attachment of m. pseudotemporalis to os suprangulare (character 131), and the origin from ossiculum supraorbitalis of m. orbicularis palpebrarum (character 144).

Although *Crypturellus* is recovered with good support, relationships within the taxon are generally weakly supported or unresolved [with the exception of the dark-coloured, relatively unpatterned clade including *Crypturellus cinereus* (Gmelin, 1789), *Crypturellus obsoletus*, *Crypturellus tataupa* (Temminck, 1815), and

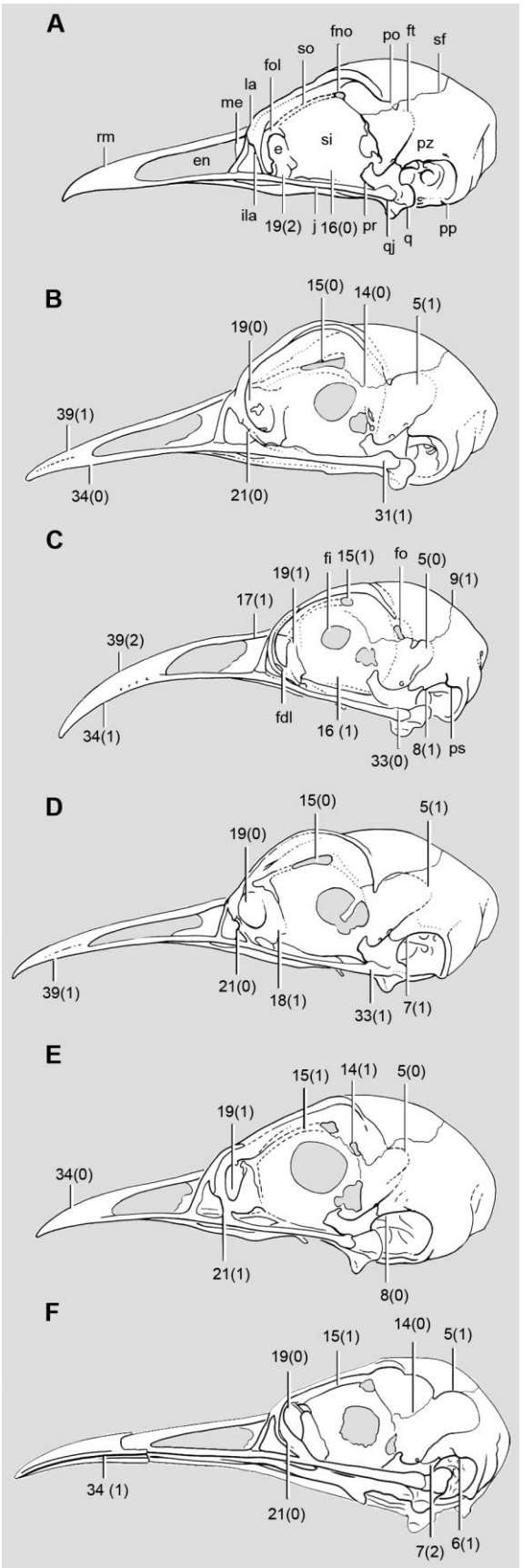

Figure 4. Skulls in lateral view: *Tinamotis pentlandii* (A); *Cypturellus soui* (B); *Nothoprocta ornata* (C); *Tinamus major* (D); *Nothura maculosa* (E); and *Rhynchotus maculicollis* (F). Abbreviations: e, os ectethmoidale; en, external nares; fi, fonticuli interorbitales; fdl, foramen ductus lacrimalis; fno, foramen n. olfactorii; fo, fonticuli orbitocraniales; fol, foramen orbitonasale laterale; ft, fossa temporalis; ila, incisura ductus lacrimalis; j, os jugale; la, os lacrimale; me, os mesethmoidale; po, processus postorbitalis; pp, processus paroccipitalis; pr, processus orbitalis; ps, prominentia supramеatica; pz, processus zygomaticus; q, os quadratum; qj, os quadratojugale; rm, rostrum maxillare; si, septum interorbitale; so, sulcus n. olfactorii; sf, sutura frontoparietalis. The numbers denote characters and character states as listed in Appendix 2. Figures are not drawn to scale.

Crypturellus parvirostris (Wagler, 1827); Fig. 1]. These results are not unexpected, given that we did not find enough anatomical information to deal specifically with interspecific relationships within *Crypturellus*. The resulting topology of the clade varied across equal and implied weight analyses: most groups with low stability in the consensus tree of the equally weighted analysis are not recovered in the weighted tree (Fig. 1). Thus, differences to the equally weighted analysis include the unresolved position of most species of *Crypturellus* (Fig. 1). In the weighted analysis, the position of *Crypturellus undulatus* (Temminck, 1815), *Crypturellus boucardi* (Sclater, 1859), and *Crypturellus soui* (Hermann, 1783) are also unresolved. The barred species *Crypturellus brevirostris* (Pelzeln, 1863), *Crypturellus bartletti* Sclater & Salvin 1873, *Crypturellus transfasciatus* (Sclater & Salvin, 1878), and *Crypturellus cinnamomeus* (Lesson, 1842) form a poorly established group that is only supported by the processus flexorius of the humerus projecting beyond the ventral condyle (character 87, Fig. 9G), with the two last species as sister groups (supported by the almost straight processus orbitalis of quadrate, character 48, Fig. 6H). Next, *Crypturellus erythropus* (Pelzeln, 1863), *Crypturellus noctivagus* (Wied-Neuwied, 1820), and *Crypturellus variegatus* (Gmelin, 1789) form a polytomy within a clade of the greyish coloured, relatively unpatterned species of *Crypturellus* (*C. cinereus*, *C. obsoletus*, *C. tataupa*, and *C. parvirostris*). The unpatterned group is recovered with relatively weak values (GC 60, Fig. 1), and is supported by a vestigial facies articularis parasphenoidalis of the mandibula (character 43, Fig. 6C), and the praeacetabular region of the pelvis being around twice or more than twice the length of the postacetabular portion (character 92). Relationships within this clade are well supported, with support values ranging from GC 82–98 (Fig. 1). The clade (*C. obsoletus* + *C. tataupa* + *C. parvirostris*) shares

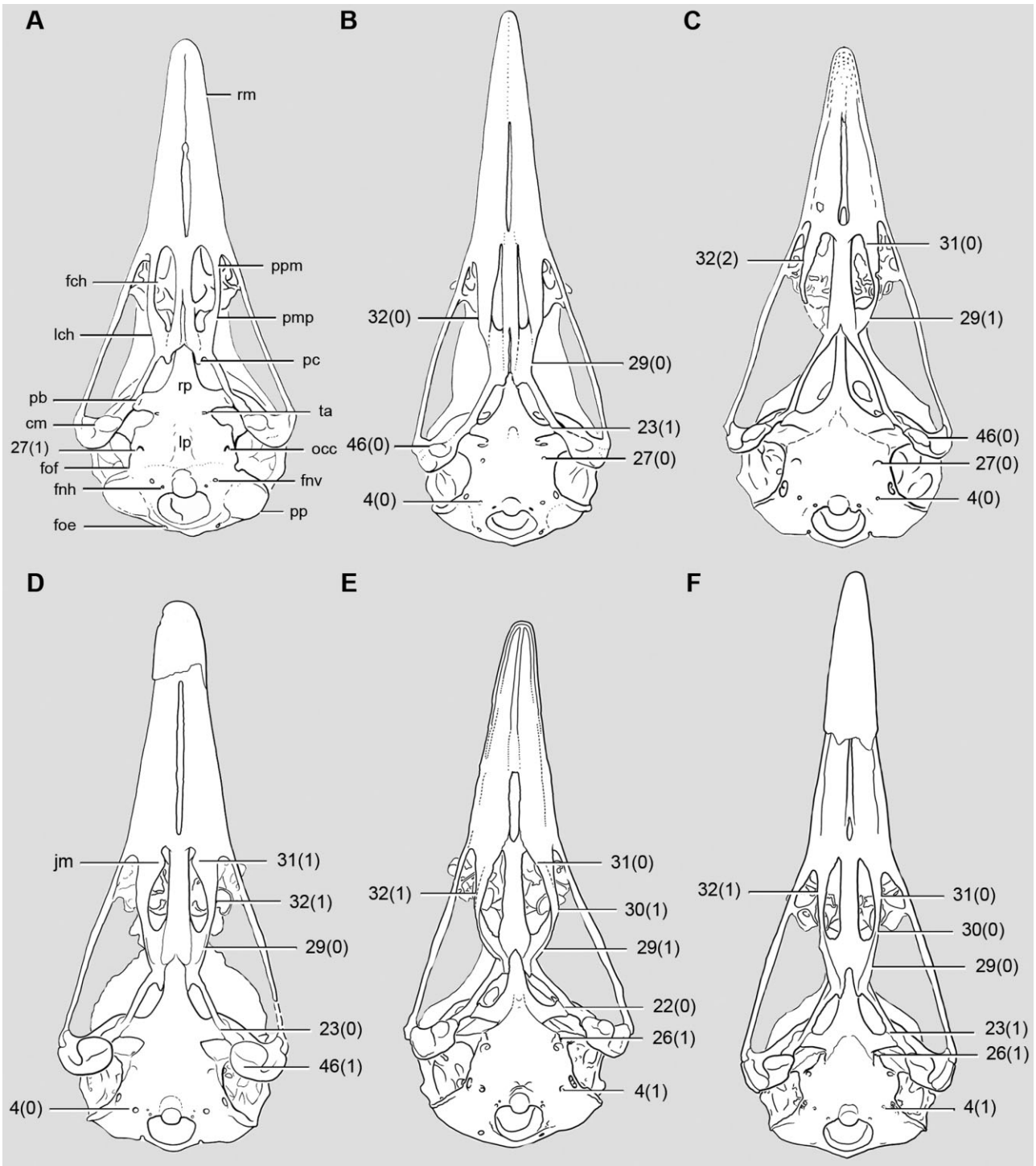

Figure 5. Skulls in ventral view: *Tinamotis pentlandii* (A); *Crypturellus cinnamomeus* (B); *Nothura minor* (C); *Eudromia formosa* (D); *Nothoprocta perdicaria* (E); and *Rhynchotus maculicollis* (F). Abbreviations: cm, condylus medialis; fch, fossa choanalis; fnh, foramen n. hypoglossi; fnv, foramen n. vagi; foe, foramen v. occipitalis externa; fof, foramen n. ophthalmici, jm, jugamentum maxillopalatinum; lch, pars choanalis (os palatinum); lp, lamina parasphenoidale; occ, ostium canalis carotici; pb, processus basipterygoideus; pc, processus caudomedialis; pmp, processsus maxillaris (os palatinum); ppm, processus maxillopalatinus (os maxillare); pp, processus paroccipitalis; rm, rostrum maxillare; rp, rostrum parasphenoidalis; ta, tuba auditiva. The numbers denote characters and character states as listed in Appendix 2. Figures are not drawn to scale.

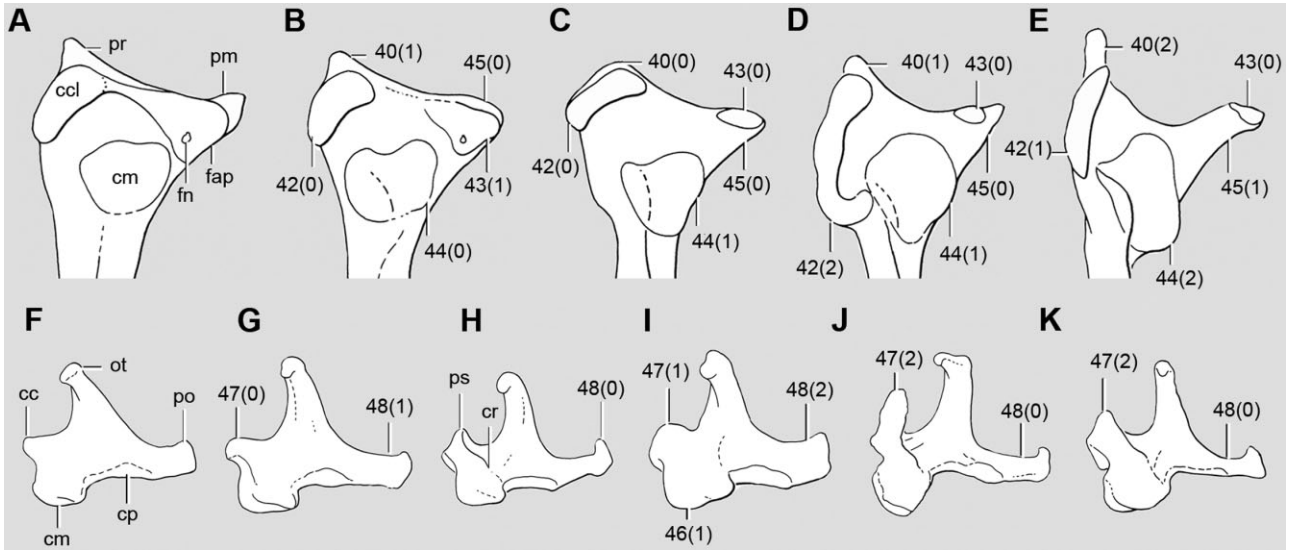

Figure 6. A–E, mandible, caudal end (dorsal view): *Tinamus major* (A); *Crypturellus cinnamomeus* (B); *Eudromia formosa* (C); *Rhynchotus maculicollis* (D); and *Nothoprocta ornata* (E). F–K, quadrate, medial view: *Nothocercus nigrocapillus* (F); *Tinamus major* (G); *Nothura darwinii* (H); *Eudromia elgans* (I); *Nothoprocta taczanowskii* (J); and *Nothoprocta perdicaria* (K). Abbreviations: cc, condylus caudalis; ccl, cotylae caudalis et lateralis; cm, condylus medialis; cp, condylus pterygoideus; cr, crest from prominentia submeatica (Elzanowski, 1987); fap facies articularis parasphenoidalis; fn, foramen pneumaticum; ot, processus oticus; pm, processus medialis mandibularis; po, processus orbitalis; pr, processus retroarticularis; ps, prominentia submeatica (Elzanowski, 1987). The numbers denote characters and character states as listed in Appendix 2. Figures are not drawn to scale.

the presence of a lacrimal duct forming a wide notch (character 21, Fig. 4E), and a well-developed cotyla medialis of the mandible (character 44, Fig. 6C and D). *Crypturellus tataupa* and *C. parvirostris* are sister taxa, which is supported by a narrow lacrimal head (character 20, Fig. 3B and D), parallel lateral grooves on the ventral mandibular surface (character 36), and a very long processus lateralis of the coracoid (character 76, Fig. 9V).

Within the open-area subtree, *Eudromia* and *Tinamotis* form a well-supported suprageneric clade (GC 99; Fig. 1), which is the sister taxon of all other nothurines. This clade is supported by myological, cranial, and postcranial evidence. The skull is characterized by a distinct fossa at the midline of the os frontale (character 10, Fig. 3C) and a wide lacrimal–ectethmoid plate that covers most of the antorbital wall (character 19, Fig. 4A). Postcranial synapomorphies of the group are: absence of processus costalis of the axis (character 52, Fig. 7B), short spina interna rostri of sternum (character 62, Fig. 8A, G), scapular blade expanding distally (character 68, Fig. 8L), coracoid with a groove for origin of ligamentum acrocoracohumerale confluent with facies articularis clavicularis (character 71, Fig. 9P), a flat processus acrocoracoideus (character 72, Fig. 9T), the proximal margin of the cotyla scapularis being perforated by large foramina (character 73, Fig. 9P), ulna distinctly longer than humerus (character 88), the crista trochanteris of the femur projecting markedly (character 100), proximal terminus of cranial rim of condylus medialis of femur subequal to proximal terminus of caudal rim (character 102, Fig. 11F), short crista cnemialis cranialis of tibiotarsus (character 105, Fig. 11N), hallux absent (character 116). Myological synapomorphies of the clade are the following: attachment of aponeurosis parabasalis to lamina basitemporalis (character 124), origin of m. adductor mandibulae externus on temporal fossa (character 126), absence of ventral portion of m. pseudotemporalis (character 130), separate m. pseudotemporalis and m. quadratomandibularis (character 132), insertion of m. quadratomandibularis beyond the dorsal margin of the mandible (character 133), complex multipennate system of pars medialis of m. pterygoideus (character 135), fasciculus caudalis of m. pterygoideus present (character 136), insertion of m. depressor mandibulae externus beyond fossa caudalis (character 139), origin from os ectethmoidale of m. levator palpebrae dorsalis (character 142), and the m. orbicularis palpebrarum formed by ligaments (character 143).

The monophyly of the taxa *Eudromia* and *Tinamotis* was also highly supported (GC 100, Fig. 1) by different types of characters. *Eudromia* is supported by a laterally compressed processus zygomaticus (character 7), an incomplete row of ossicles supraorbitalis

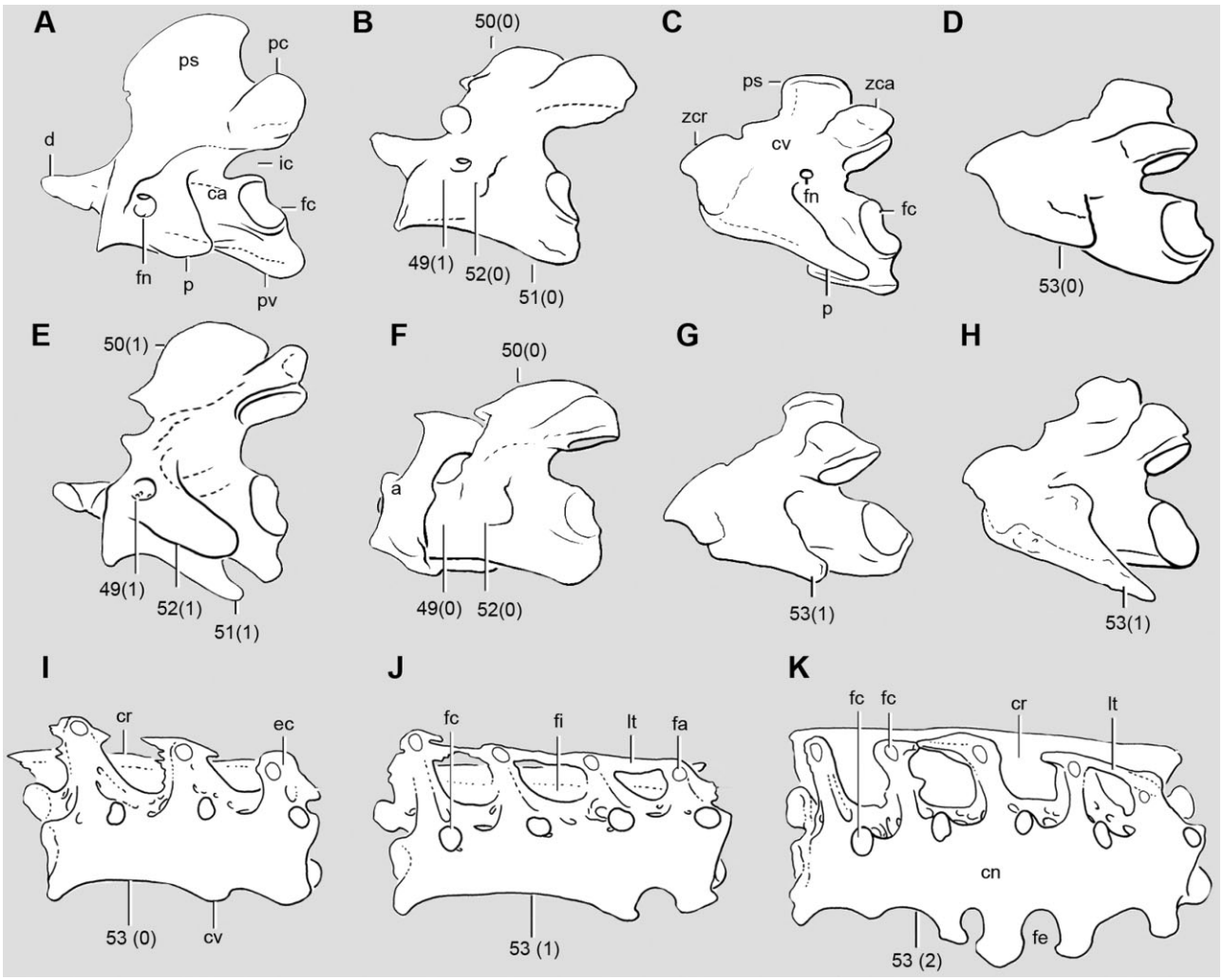

Figure 7. A, B, E, F, axis, left lateral side: *Rhynchotus maculicollis* (A); *Eudromia elegans* (B); *Nothoprocta pentlandii* (E); and *Tinamotis pentlandii* (articulated with atlas, F). C, D, G, H, cervical vertebra 3, left lateral view: *Rhynchotus maculicollis* (C); *Tinamotis pentlandii* (D); *Eudromia elegans* (G); *Nothoprocta pentlandii* (H). I–K, notarium (lateral view): *Nothocercus bonapartei* (I); *Tinamus solitarius* (J); and *Nothoprocta taczanowskii* (K). Abbreviations: a, atlas; ca, corpus axis; cn, corpus notarii; cr, crista spinosa notarii; cv, corpus vertebrae; d, dens; ec, eminentia costolateralis; fa, facies articularis costalis fc, facies articularis caudalis; fe, fenestra intercristalis; fi, fenestra intertransversaria; fn, foramen pneumaticum; ic, incisura caudalis; lt, lamina transversa notarii; p, processus costalis; pc, processus articularis caudalis; ps, processus spinosus; pv, processus ventralis; zca, zygapophysis caudalis; zcr, zygapophysis cranialis. The numbers denote characters and character states as listed in Appendix 2. Figures are not drawn to scale.

(character 12, Fig. 3C), presence of a jugamentum maxillopalatinum of os palatinum (character 31, Fig. 5D), a mediolaterally wide processus maxillopalatini (wider than fossa choanalis; character 32, Fig. 5D), processus retroarticularis of mandibula absent (character 40, Fig. 6C), inflated aspect of medial area (between articular condylae) of os quadratum (character 46, Fig. 6I), coracoid with overhanging tuberculum brachiale (character 70, Fig. 9Q), condylus lateralis of tibiotarsus distinctly longer than condylus medialis (character 104, Fig. 11H, L), broad hypotarsal sulcus/canal for m. flexor digitorum longus (character 111, Fig. 12H), absence of sharp medial ridge at the cotyla medialis of tarsometatarsus (character 112; Fig. 12H), presence of ligamentum sphenomandibulare (character 123), and strongly developed aponeurotic sheet of m. quadratomandibularis (character 134). *Tinamotis* is supported by the following osteological and myological synapomorphies: a caudally placed ostium canalis carotici (character 27, Fig. 5A), a rostrocaudally narrow pars choanalis of the os palatinum (character 29, Fig. 5A), a distinct facies articularis parasphenoidalis

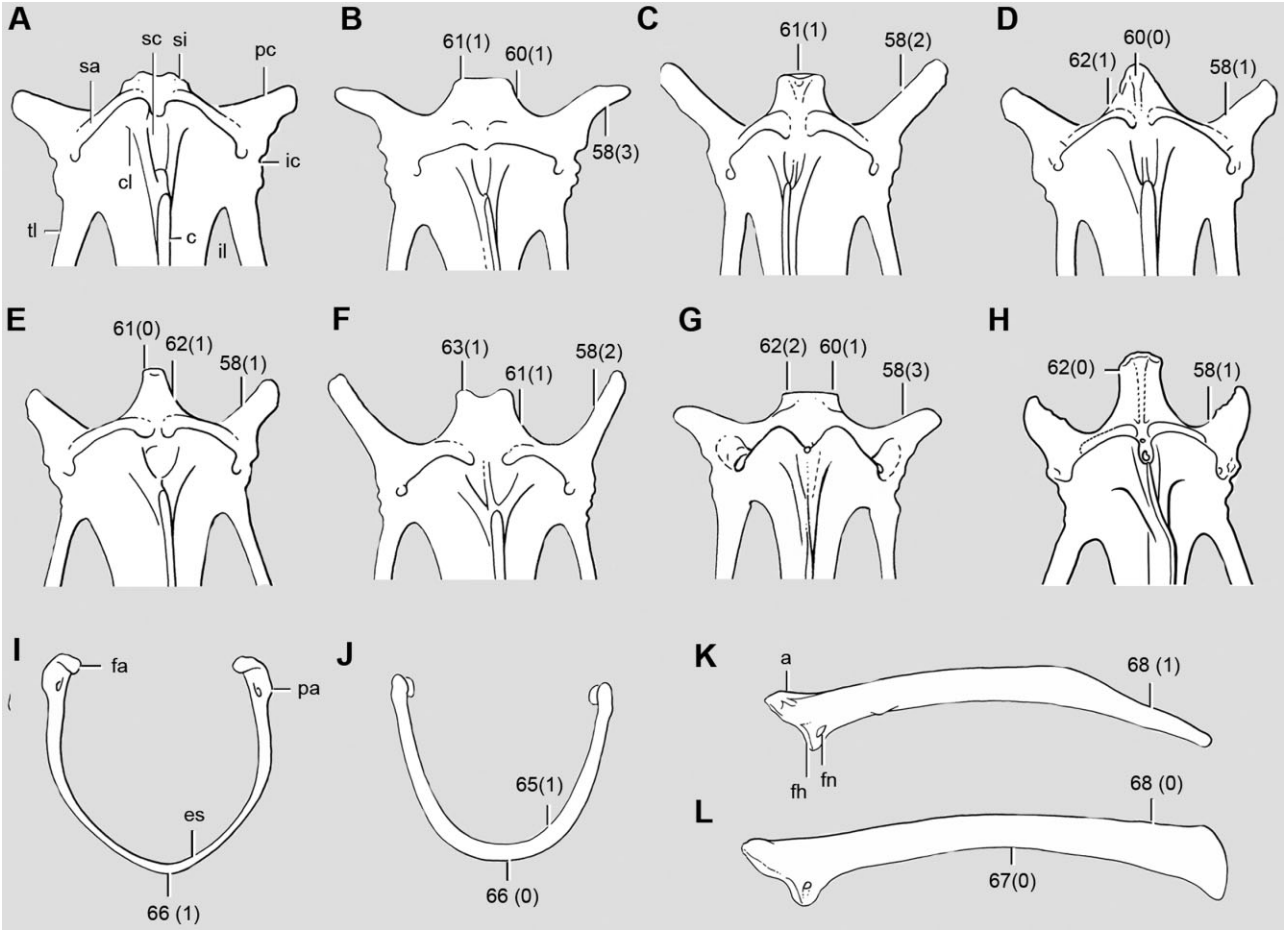

Figure 8. A–H, sternum, ventral view, proximal end: *Eudromia elegans* (A); *Nothocercus julius* (B); *Nothura maculosa* (C); *Nothoprocta cinerascens* (D); *Crypturellus erythropus* (E); *Taoniscus nanus* (F); *Tinamotis pentlandii* (G); and *Tinamus major* (H). I, J, clavicula of *Nothoprocta pentlandii* (caudal view; I) and *Crypturellus brevirostris* (cranial view; J). K, L, scapula (medial view) of *Nothoprocta pentlandii* (K) and *Tinamus major* (L). Abbreviations: a, acromion; c, carina sterni; cl, crista lateralis carinae; es, extremitas sternalis claviculae; fa, facies articularis acrocoracoidea; fh, facies articularis humeralis; fn, foramen pneumaticum; ic, incisura intercostalis; il, incisura lateralis; pa, processus acromialis; pc, processus craniolateralis; sa, sulcus articularis coracoideus; sc, sulcus carinae; si, spina interna; tl, trabecula lateralis. The numbers denote characters and character states as listed in Appendix 2. Figures are not drawn to scale.

(character 43, Fig. 6B), corpus of axis without pneumatic foramina on lateral sides (character 49, Fig. 7F), absent or poorly projected processus costales on first series of vertebrae cervicales (character 53, Fig. 7D), humerus with shorter or subequal ventral condyle relative dorsal condyle (character 83, Fig. 9B), and processus supracondylaris ventralis cranially located (character 86, Fig. 9B), distal end of radius expanded (character 89, Fig. 9M), a very wide pelvis (character 98, Fig. 10H), a vestigial foramen vasculare distale of the tarsometatarsus (character 114, Fig. 12I), and both trochleae II and IV of the tarsometatarsus being about equally projected distally (character 115, Fig. 12I).

The clade consisting of *Taoniscus*, *Nothura*, *Nothoprocta*, and *Rhynchotus* is recovered with high support (GC 95; Fig. 1). A vestigial temporal notch (character 5, reversed in *Rhynchotus*; Fig. 4C, E), large fonticuli orbitocraniales (character 14, Fig. 4C, E), a long and curved processus orbitalis of the quadratum (character 48, Fig. 6H, J, K), and an elongated cotyla medialis of the mandibula (character 44, Fig. 6D, E) are characteristic features of the skull of the members of this clade. The postcranium also displays several diagnostic characters: the synsacrum has a distinctly depressed dorsal surface (character 56, Fig. 10I) and a flat centrum, with incompletely fused processus costales (character 48, Fig. 10J), the sternum possesses greatly elongated processus craniolaterales (character 58, Fig. 8C, F), the carpometacarpus has rounded caudal rims with deep infratrochlear pits (character 91, Fig. 9J), the pelvis

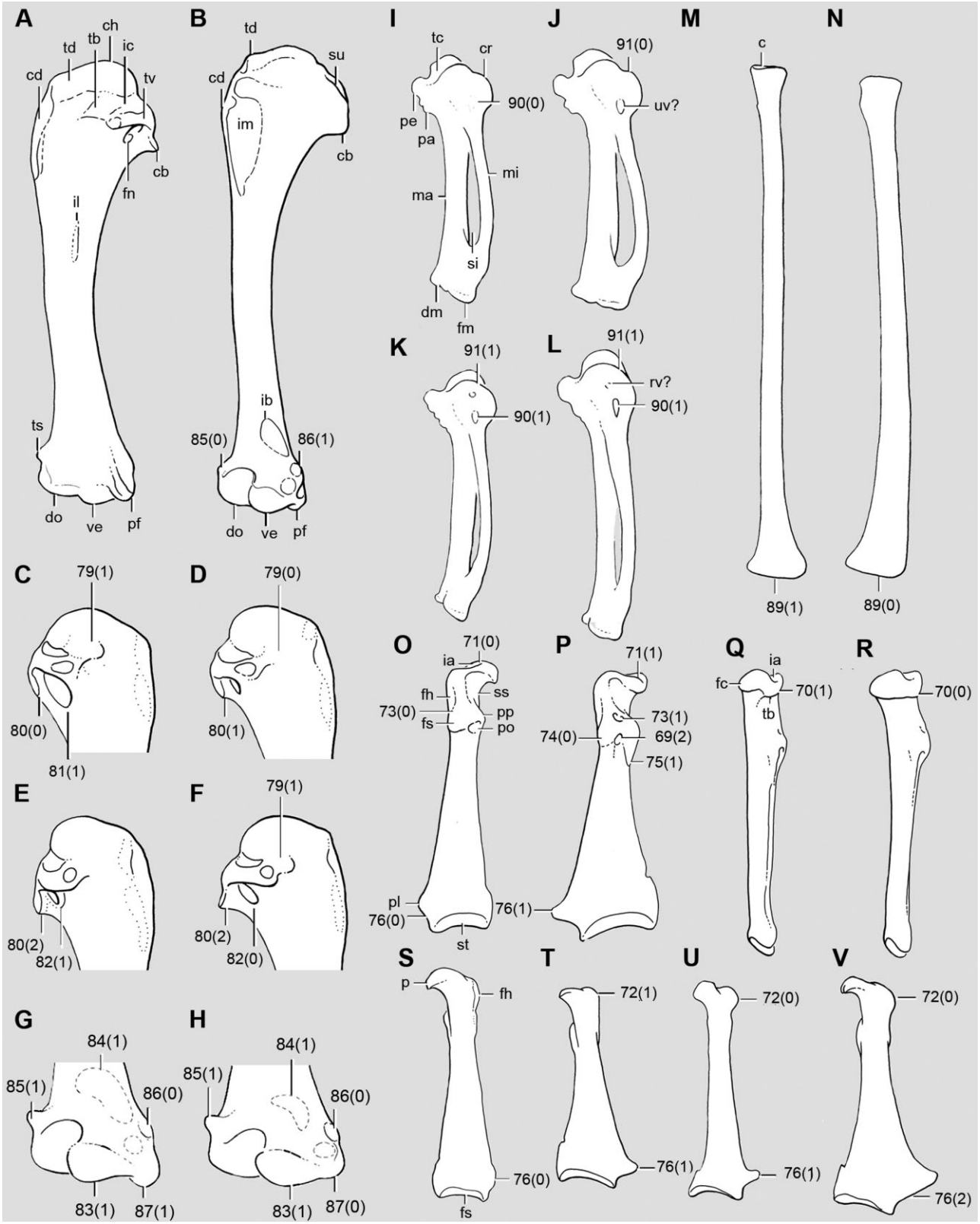
A
ch
td
tb
ic
cd
tv
cb
fn
il
ts
do
ve
pf
B
td
su
cd
im
cb
ib
85(0)
86(1)
do
ve
pf
I
tc
cr
90(0)
pe
pa
mi
ma
si
dm
fm
J
91(0)
uv?
M
c
89(1)
N
89(0)
K
91(1)
90(1)
L
91(1)
rv?
90(1)
C
79(1)
80(0)
81(1)
D
79(0)
80(1)
E
80(2)
82(1)
F
79(1)
80(2)
82(0)
G
84(1)
85(1)
86(0)
83(1)
87(1)
H
84(1)
85(1)
86(0)
83(1)
87(0)
O
71(0)
ia
fh
ss
73(0)
pp
fs
po
pl
76(0)
76(1)
st
P
71(1)
73(1)
74(0)
69(2)
75(1)
Q
ia
fc
70(1)
tb
R
70(0)
S
p
fh
76(0)
fs
T
72(1)
76(1)
U
72(0)
76(1)
V
72(0)
76(2)

Figure 9. A, B, humerus of *Crypturellus soui* (caudal view, A) and *Tinamotis pentlandii* (cranial view, B). C–F, humerus, proximal end (caudal view): *Megapodius freycinet* (C); *Tinamus major* (D); *Rhynchotus maculicollis* (E); *Crypturellus soui* (F). G, H, humerus, distal end (cranial view) of *Crypturellus erythropus* (G) and *Crypturellus tataupa* (H). I–L, carpometacarpus, ventral view: *Nothocercus julius* (I); *Cypturellus soui* (J); *Nothura minor* (K); and *Rhynchotus maculicollis* (L). M, N, radius, ventral view of *Tinamotis pentlandii* (M) and *Tinamus tao* (N). O, P, coracoid, dorsal view, of *Nothocercus bonapartei* (O) and *Crypturellus barletti* (P). Q, R, coracoid, medial view, of *Tinamotis pentlandii* (Q) and *Crypturellus undulatus* (R). S–V, coracoid, ventral view, of *Nothocercus julius* (S), *Crypturellus bartletti* (T), *Taoniscus nanus* (U), and *Nothoprocta cinerascens* (V). Abbreviations: c, cotyla humeralis; cb, crista bicipitalis; cd, crista deltopectoralis; ch, caput humeri; cr, caudal rim of trochlea carpalis; dm, facies articularis digitalis major; do, condylus dorsalis; fc, facies articularis clavicularis; fh, facies articularis humeralis; fm, facies articularis digitalis minor; fn, fossa pneumotricipitalis; fs, facies articularis scapularis; ia, impressio ligamentum acrocoracohumeralis; ic, incisura capitis: ib, impressio m. brachialis; il, impressio m. latissimi dorsi; im, impressio coracobrachialis; ma, os metacarpale majus; mi, os metacarpale minus; p, processus acrocoracoideus; pa, processus alularis; pe, processus extensorius; pf, processus flexorius; pl, processus lateralis; po, pneumatic opening; pp, processus procoracoideus; rv, attachment of ligamentum radiometacarpalis ventralis; si, spatium intermetacarpale; ss, sulcus m. supracoracoidei; st, facies articularis sternalis; su, sulcus transversus; tb, tuberculum brachiale; tc, trochlea carpalis; td, tuberculum dorsale; ts, processus supracondylaris dorsalis; tv, tuberculum ventrale; uv, attachment of ligamentum ulnometacarpalis ventralis; ve, condylus ventralis. The numbers denote characters and character states as listed in Appendix 2. Figures are not drawn to scale.

is characterized by a praeacetabular area that has twice or more the length of the postacetabular portion (character 92, Fig. 10E, F), an illium with expanded cranial (character 94, Fig. 10I, J) and caudal (character 97, Fig. 10I, J) ends, and a well-projected tuberculum praeacetabulare (character 99; Fig. 10E, F).

Within this group, *Taoniscus nanus* (Temminck, 1815) is sister taxon of a paraphyletic *Nothura*, with the species *Nothura minor* (Spix, 1825), *Nothura boraquira* (Spix, 1825), *Nothura maculosa* (Temminck, 1815), and *Nothura darwinii* (G.R. Gray, 1867) being successive sister taxa (although minimally supported) of a clade formed by *Rhynchotus* and a monophyletic *Nothoprocta*, also recovered with high support (GC 99; Fig. 1). This clade (*Rhynchotus* + *Nothoprocta*; Fig. 1) is supported by a large number of cranial features and a unique postcranial character (character 103: distinctly bowed femora, Fig. 11A). Cranial synapomorphies of these taxa include: a long and curved sulcus v. occipitalis externa (character 1, Fig. 3G, H), a foramen n. vagi placed near to foramen n. ophthalmici (character 4, Figs 3G–H and 5F), the presence of a lacrimal foramen (character 21, Fig. 4C, F), bony processes next to the ostium canalis carotici (character 26, Figs 3G, H and 5F), vestigial processes of os quadratojugale (character 33, Fig. 4C, F), markedly decurved ramus mandibularis (character 39, Fig. 4C, F). This relationship is also diagnosed by several myological features: the attachment of aponeurosis parabasalis to lamina basitemporalis (character 124), a partially tripartite m. adductor mandibulae externus (character 128), the absence of a ventral temporal portion of m. pseudotemporalis (character 130), the insertion of m. quadratomandibularis beyond the dorsal margin of the mandible (character 133), three unipennate portions (character 135), a fasciculus caudalis (character 136), and fused aponeuroses of the pars medialis of m. pterygoideus (character 137).

The monophyly of *Rhynchotus* is highly supported (GC 99, Fig. 1) by the following synapomorphies: a marked crista nuchalis sagittalis (character 2, Fig. 3H), prominent processus paraoccipitalis (character 3, Fig. 3H), a large fossa temporalis (character 5, Fig. 4F), notched ventral margin of the processus zygomaticus (character 8, Fig. 4F), a broad interorbital area of os frontale (character 13, Fig. 3C), a narrow lacrimal–ectethmoid complex (character 19, Fig. 4F), a rostrocaudally wide pars choanalis of os palatinum (character 29, Fig. 5F), absence of lateral grooves of maxilla and mandibula (character 35), long and strongly curved cotyla lateralis and caudalis of mandibula (character 42, Fig. 6D), tibiotarsus, condylus lateralis distinctly longer than medialis (character 104; Fig. 11H, L).

Nothoprocta is also recovered with good support (GC 95, Fig. 1). Synaporphies of the clade include the processus maxillaris of os palatinum being distinctly curved and facing ventrally (character 30, Fig. 5E), deep and craniocaudally elongated cotyla medialis of mandibula (character 44, Fig. 6E), blade-like processus ventralis of axis (character 51, Fig. 7E), absence of ligamentum quadratomandibulare rostrale (character 121), and origin of m. obliquus dorsalis divided into three parts (character 146). Within the genus, *Nothoprocta cinerascens* (Burmeister, 1860) is the sister taxon of all other species of the genus, i.e. *Nothoprocta taczanowskii* (Sclater & Salvin, 1875), *Nothoprocta pentlandii* Gray, 1867, *Nothoprocta ornata* (G.R. Gray, 1867), and *Nothoprocta perdicaria* (Kittlitz, 1830), which form a clade of successive sister taxa, although recovered with a considerable level of conflict (Fig. 1). The

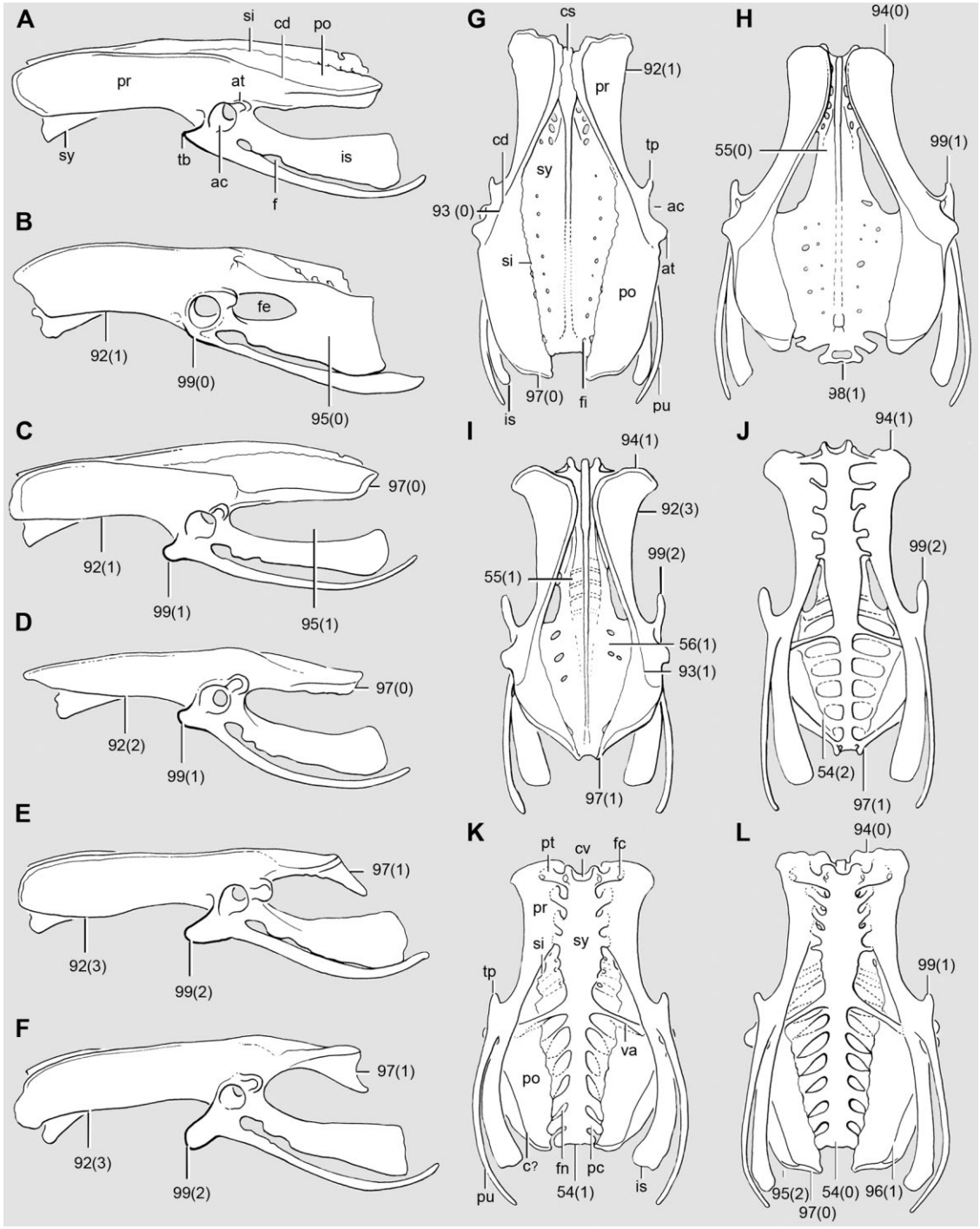

Figure 10. A–F, pelvis, lateral view: *Crypturellus cinnamomeus* (A); *Megapodius freycinet* (B); *Tinamus solitarius* (C); *Nothocercus bonapartei* (D); *Nothoprocta perdicaria* (E); and *Nothoprocta taczanowskii* (F). G–I, pelvis, dorsal view: *Tinamus solitarius* (G); *Tinamotis pentlandi* (H); and *Nothura darwinii* (I). J–L, pelvis, ventral view: *Nothura darwinii* (J); *Crypturellus cinnamomeus* (K); and *Tinamus solitarius* (L). Abbreviations: ac, foramen acetabuli; at, antitrochanter; c, crista for attachment of ilioischiatic membrane; cd, crista dorsolateralis ilii; cs, crista spinosa synsacri; cv, corpus vertebrae; f, fenestra ischiopubica; fc, fovea costalis; fe, foramen ilioischiadicum; fi, foramina intertransversaria; fn, fenestra intertransversaria; is, ischium; pc, processus costalis; pr, ala praeacetabularis ilii; po, ala postacetabularis ilii; pt, processus transversus; pu, pubis; si, sutura iliosynsacralis; sy, synsacrum; tb, tuberculum praeacetabulare; va, vertebra acetabularis. The numbers denote characters and character states as listed in Appendix 2. Figures are not drawn to scale.

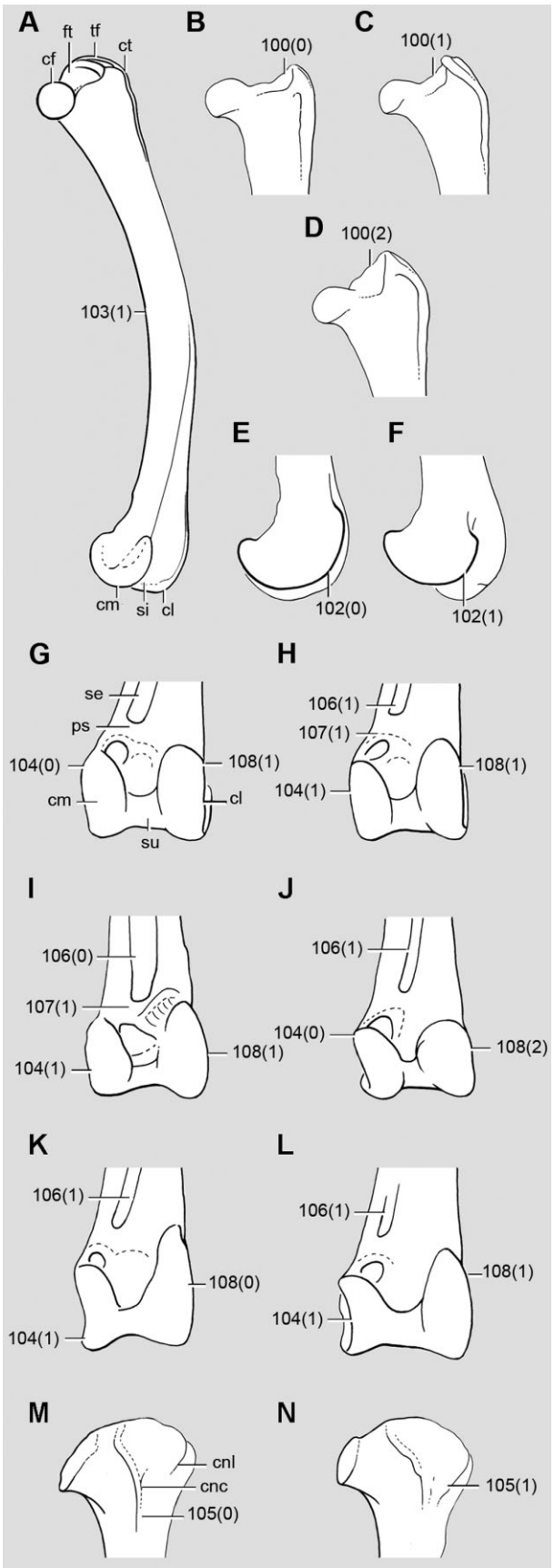

Figure 11. A, femur, craniomedial view, of *Nothoprocta taczanowskii*. B–D, femur, proximal end (cranial view): *Megapodius freycinet* (B); *Nothoprocta ornata* (C); and *Tinamus tao* (D). E, F, femur, distal end (medial view) of *Rhynchotus maculicollis* (E) and *Tinamotis pentlandii* (F). G–L, tibiotarsus, distal end (cranial view): *Nothoprocta perdicaria* (G); *Rhynchotus maculicollis* (H); *Megapodius freycinet* (I); *Tinamotis penlandii* (J); *Tinamus tao* (K); and *Eudromia elegans* (L). M, N, tibiotarsus, proximal end (cranial view) of *Tinamus tao* (M) and *Tinamotis pentlandii* (N). Abbreviations: cf, caput femoris; cl, condylus lateralis; cm, condylus medialis; cnc, crista cnemialis cranialis; cnl, crista cnemialis lateralis; ct, crista trochanteris; ft, fossa trochanteris; ps, pons supratendineus; se, sulcus extensorius; si, incisura intercondylaris; su, sulcus intercondylaris; tf, trochanter femoris. The numbers denote characters and character states as listed in Appendix 2. Figures are not drawn to scale.

clade (*N. taczanowskii* + *N. pentlandii* + *N. ornata* + *N. perdicaria*) is supported by the presence of caudally divergent lateral grooves of the mandibular plates (character 36), markedly decurved ramus mandibularis (character 39), long and narrow processus medialis mandibularis (character 45, Fig. 6E), and a notarium with five fused vertebrae (character 57, Fig. 7K). The presence of a projected processus retroarticularis of the mandibula (character 40, Fig. 6E) supports (*N. pentlandii* + *N. ornata* + *N. perdicaria*), and the clade (*N. ornata* + *N. perdicaria*) shares a processus craniolateralis of the sternum that is less projected than the spina interna (character 58, Fig. 8D, H) and the proximal margin of the cotyla scapularis being perforated with large foramina (character 73, Fig. 9P).

Phylogenetic placement of extinct taxa

The strict consensus tree including the extinct fossil tinamous exhibits a large polytomy involving all species of Tinamidae; however, this is only because of the unstable position of the fragmentary early Miocene terminals MACN-SC-T and MACN-SC-H, and the extinct species *Crypturellus reai* and *Nothura* sp. The unstable behaviour of the early Miocene fossils is related to the limited information (i.e. missing data) and not to conflicting scorings; however, in spite of the incomplete evidence, the identification of these fossils is based on the presence of diagnostic apomorphies of Tinamidae (a ventral condyle of the humerus with its main axis longer than the dorsal condyle and a round and prominent dorsal supracondylar process, and a medially placed extensor canal of tibiotarsus covered by an ossified supratendinal bridge; Fig. 1). In contrast, the unstable position in the tree of the early Miocene *Crypturellus reai* and the Pleistocene *Nothura* sp. results from a combination of missing data and character conflict.

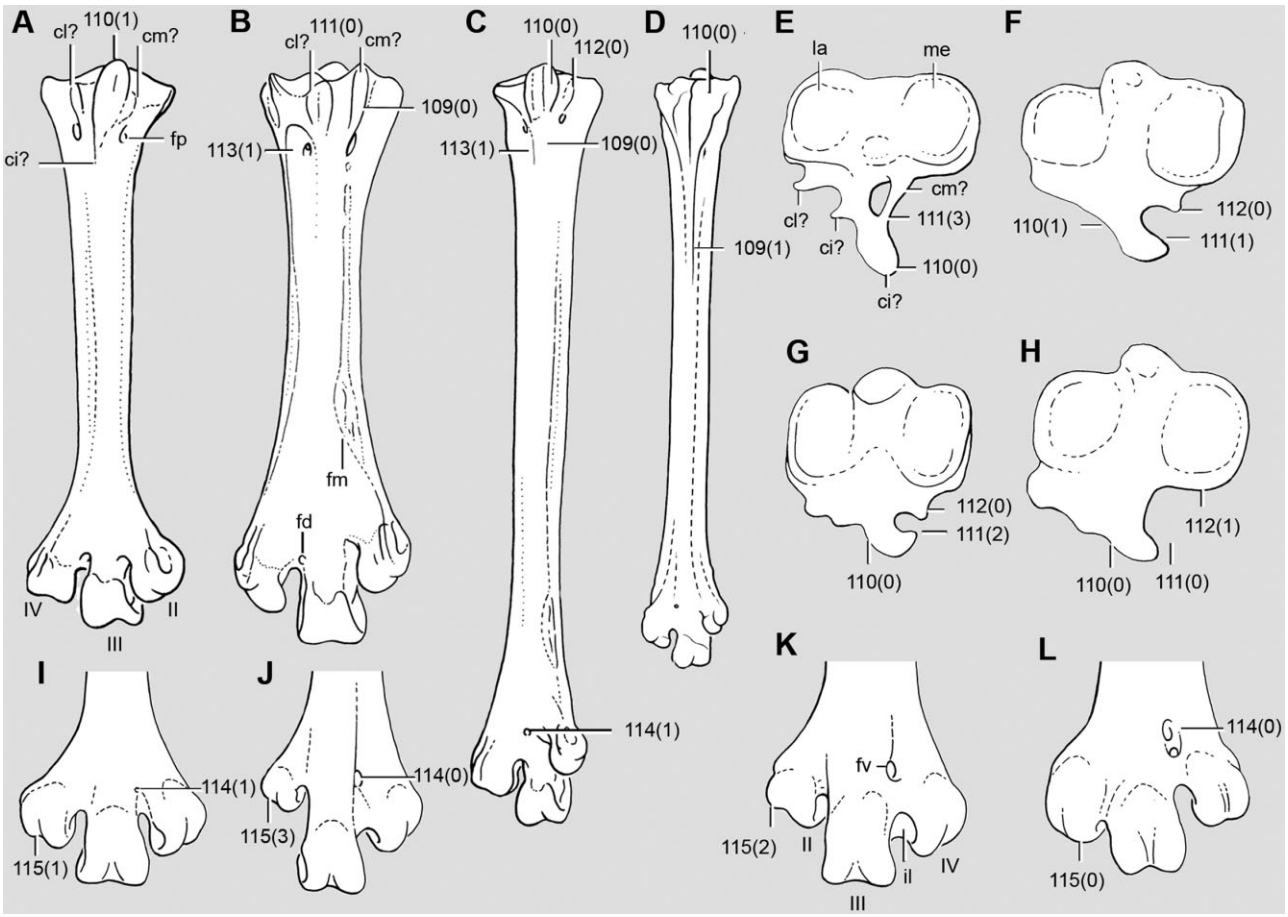

Figure 12. A–D, tarsometatarsus, plantar view: *Tinamotis pentlandii* (A); *Apteryx australis* (B); *Nothocercus bonapartei* (C); and *Crypturellus erythopus* (D). E–H, tarsometatarsus, proximal view: *Megapodius freycinet* (E); *Tinamotis pentlandii* (F); *Crypturellus soui* (G); and *Eudromia elegans* (H). I–L, tarsometatarsus, distal end (dorsal view): *Tinamotis pentlandii* (I); *Rhynchotus rufescens* (J); *Eudromia elegans* (K); and *Megapodius freycinet* (L). Abbreviations: ci, crista intermedia hypotarsi; cl, crista lateralis hypotarsi; cm, crista medialis hypotarsi; fp, foramen vasculare proximale; fd, foramen vasculare distale; fm, fossa metatarsi I; fv, foramen vasculare distale; il, incisura intertrochlearis lateralis; II, trochlea metatarsi II; III, trochlea metatarsi III; IV, trochlea metatarsi IV; la, cotyla lateralis; me, cotyla medialis. The numbers denote characters and character states as listed in Appendix 2. Figures are not drawn to scale.

Given that these terminals are identified as responsible for a great deal of instability, they were excluded a posteriori from the consensus tree of the heuristic searches. Such a procedure tests the interrelationships of tinamous (living and fossil taxa), by comparing sets of phylogenetic trees inferred from all the available data (i.e. including those fossils of ambiguous position; Pol & Escapa, 2009). The reduced consensus resulting after the exclusion of MACN-SC-T, MACN-SC-H, *Crypturellus reai*, and *Nothura* sp. shows a high degree of resolution, and is used here to summarize the results of our phylogenetic study (Fig. 1).

Support values for the placements of fossil terminals are low, even when ignoring the alternative positions of the unstable MACN-SC-T, MACN-SC-H, *Crypturellus reai*, and *Nothura* sp. (Fig. 1). Because the fossils feature many missing entries, several derived character states optimized as synapomorphies in the consensus cladogram of the extant species are not unambiguously optimized in all shortest trees. This effect is not caused by homoplasy but by the ambiguity resulting from the limited evidence provided by the incomplete fossils. For example, the earliest known tinamous are fragmentary postcranial elements: the tibiotarsi of MACN-SC-T show multiple positions within Tinamidae in all optimal topologies and the humeri of MACN-SC-H fall in alternative positions within Tinaminae (Fig. 1).

Although the clade support values are low, the placement of the remaining early Miocene fossils is well resolved given the high percentage of missing data for these terminal units (Fig. 1). The coracoids MACN-

SC-3610 and MACN-SC-3613 share with those of living species of tinamous the presence of a large foramen on the dorsal surface of the bone, distal to the articular facet for the scapula. Unlike the humeri and tibiotarsi, these remains show derived character states that support branches within the clade Tinaminae: the early Miocene coracoids MACN-SC-3610 and MACN-SC-3613 are thus placed within the forest-dwelling tinamous, as the sister taxa of the extant *Crypturellus*. Supporting character evidence for this relationship includes the lack of a cranially projected processus acrocoracoideus and the presence of a foramen perforating the upper margin of the scapular facet. The extinct species *Crypturellus reai* shows multiple positions within *Crypturellus*, results that are congruent with the previously proposed relationships of the fossil (Chandler, 2012).

With the exception of the early Miocene specimens, most Tertiary fossils fall within the open-area Nothurinae in all the most parsimonious cladograms. The late Miocene *Eudromia* sp. is positioned outside the clade including *Eudromia* and *Tinamotis* (Fig. 1). Most of the coded character states of the coracoid are unknown in the coracoid of *Eudromia* sp. and therefore are currently optimized as ambiguous apomorphies of this node; however, the coracoid of the species of the (*Eudromia* + *Tinamotis*) clade lacks a cranially projected processus acrocoracoideus, an unambiguous apomorphy absent in *Eudromia* sp., in which the process is cranially projected.

The phylogenetic placement of the Pliocene tinamou species *Eudromia olsoni* and *Nothura parvula* is consistent with their original assignment (Fig. 1). The placement of *Eudromia olsoni* within the extant *Eudromia* clade is supported by the presence of a coracoid with a crescent-shaped facies articularis clavicularis and an overhanging tuberculum brachiale.

Nothura parvula is nested within the extant *Nothura*, depicted in the reduced consensus tree as a paraphyletic taxon with respect to the (*Nothoprocta* + *Rhynchotus*) clade (Fig. 1). This position is supported by the presence of pneumatic openings on the impression for the m. sternocoracoidei of the coracoid and a rounded and compact processus supracondylaris dorsalis of the humerus. Furthermore, the femur of the (*Rhynchotus* + *Nothoprocta*) clade exhibits a strongly curved shaft, an unambiguous apomorphy absent in *Nothura parvula*.

The Pleistocene *Nothura* sp. (excluded from the consensus a posteriori) takes multiple positions within the open-area taxa *Taoniscus*, *Nothura*, and *Nothoprocta* (Fig. 1). This uncertainty is related to both a lack of morphological data (missing entries) for critical characters and conflict in the character-state distribution in the unstable position of the fossil; however, its original identification as *Nothura* sp. is not contradicted by the present analysis.

DISCUSSION

The current analysis of osteological and myological characters recovered a tree structure similar to the molecular study of Porzecanski (2003): the open-area and forest-dwelling tinamous form monophyletic groups in all most-parsimonious hypotheses (see Fig. 1). Therefore, the early classification of Nothurinae (open-area tinamous) and Tinaminae (forest-dwelling tinamous) proposed by Miranda-Ribeiro (1937) is confirmed in the present analysis. The monophyly of the currently recognized polytypic tinamou genera is also recovered with high support: only *Nothura* is recovered as paraphyletic.

The monophyly of the open-area tinamous has been consistently supported by integumentary (Bertelli *et al*., 2002; Bertelli & Giannini, 2013), molecular (Porzecanski, 2003), and less inclusive osteological data sets (Bertelli & Chiappe, 2005). In the present analysis we added twice as many osteological and myological characters, increasing support for the monophyly of this entire clade, most polytypic genera (except for *Nothura*), and nothurine suprageneric clades.

Within Nothurinae, the recovered sister-group relationship between the clades (*Eudromia* + *Tinamotis*) and (*Taoniscus* (*Nothura* (*Nothoprocta* + *Rhynchotus*))) (Fig. 1) is also congruent with the molecular analysis of Porzecanski (2003), but such a relationship was previously not recovered in other morphological studies (Bertelli *et al*., 2002; Bertelli & Chiappe, 2005; Bertelli & Giannini, 2013). A sister-group relationship between *Tinamotis* and *Eudromia*, by contrast, is uncontroversial, and has been recognized for over a century (Salvadori, 1895); the basal position of these taxa within Nothurinae has, however, not been suggested by previous morphological studies. The present analysis further recovered a clade formed by the remaining open-area tinamous (*Taoniscus*, *Nothura*, *Nothoprocta*, and *Rhynchotus*). Given the absence of information on *Taoniscus*, myological apomorphies provide unambiguous support for this clade in only some of the optimal trees.

Despite the generally low support values for the basal nodes within Nothurinae (and contrary to previous morphological analyses that recovered *Rhynchotus* as closed related to *Tinamotis* + *Eudromia*; see Bertelli *et al*., 2002; Bertelli & Chiappe, 2005; Bertelli & Giannini, 2013), the clade (*Rhynchotus* + *Nothoprocta*) (Fig. 1) is robustly supported by unambiguous osteological apomorphies. An additional contribution of the present study was the recovery of a monophyletic forest-dwelling clade (Fig. 1), a group that previously had been only supported by molecular evidence (Porzecanski, 2003). Paraphyly of Tinaminae was previously suggested, albeit weakly supported, and with considerable character conflict, in studies based on external morphology (Bertelli *et al*., 2002; Bertelli & Giannini,

2013) and osteology (Bertelli & Chiappe, 2005), which placed the forest genera at the base of the tinamou tree and sequentially related to Nothurinae. The topology of the forest-dwelling tinamous section of the tree resulting from our analysis is identical to the molecular hypothesis of Porzecanski (2003), recovering *Nothocercus* outside the (*Tinamus* + *Cypturellus*) clade (Fig. 1).

In summary, osteological data were shown to support most nodes within the phylogenetic tree of tinamous. Myological characters also contribute to the support of several nodes, but a number of muscular traits included in the current analysis could not be optimized as synapomorphies because of a lack of information for some taxa (e.g. Tinaminae). Overall, the new data bring considerable additional evidence in support of well-established groups (Fig. 1).

The MPTs resulting from the present analysis suggest two major divergences within Tinamidae: a group of forest-dwelling taxa and an open-area clade (Figs 1 and 2). Some anatomical modifications are likely to be related to feeding adaptations, flight, and/or terrestrial locomotion. Future studies on the possible functional relationship among these transformations will be crucial for understanding the morphological evolution of tinamous. Morphological features of the skull, such as the projection of the prominentia submeatica of the quadrate (Elzanowski, 1987) and modifications of the mandibular articular area, are markedly developed in the open-area groups (Fig. 2). Although tinamous are mainly terrestrial birds, most open-area species (e.g. *Taoniscus*, *Nothura*, *Nothoprocta, Rhynchotus*, and *Eudromia*) have greater flight capabilities than their forest-dwelling relatives, and often engage in short flights alternating between gliding periods (Fjeldså & Krabbe, 1990). The marked increase in the size of the processus lateralis of the coracoid and the processus craniolateralis of the sternum, and other notable changes in the pectoral girdle (e.g. characters 57, 58, 66, 75, 76), may be related to the increased flight capabilities of the open-area tinamous (Fig. 2).

The postacetabular pelvis of most forest-dwelling tinamous is similar or more developed than the praeacetabular area, as opposed to the markedly longer praeacetabular pelvis (and tuberculum praeacetabulare) of the open-area groups (Fig. 2). The postacetabular part of the pelvis is the main area of origin of muscles that insert on the distal femur and proximal tibiotarsus (e.g. m. iliotibialis and m. iliotrochantericus; Hudson *et al*., 1972), and changes of the development of the postacetabular pelvis could be related to differences in the cursorial ability and running patterns of tinamous. The known fossil record of tinamous is restricted to the early Miocene–Quaternary interval of southern South America. The earliest tinamous are about 16.5 million years old and are, in our analysis, placed within both the open-area and the forest-dwelling groups. The age of these fossils, together with the monophyly of Nothurinae and Tinaminae supported from the present study, indicate that the divergence of tinamous into those of open areas and those of forests is at least 16.5 million years old. Palaeoenvironmental studies document subtropical conditions for the early Miocene of southern Argentina (Bown & Larriestra, 1990; Genise & Bown, 1994; Vizcaíno, Kay & Bargo, 2012). The flora and fauna, in particular primates, marsupials, porcupines, and rodents (Tejedor, 2002; Kay *et al*., 2012; Abello, Ortiz Jaureguizar & Candela, 2012; Brea, Zucol & Iglesias, 2012; Vizcaíno *et al*., 2012), point to the existence of forests growing under warm, humid conditions. Palaeoenvironmental inferences of younger depositional sequences indicate the development of periodically drier areas and more open environments (Vizcaíno *et al*., 2012). The oldest known fossil tinamous thus appear to have existed at a time when the early Miocene subtropical forested landscapes of southern South America were transitioning into the open-area environments that characterize most of the region today. With the exception of these early–middle Miocene fossils, most of the younger records of tinamous are more closely related to the open-area Nothurinae (Fig. 1). Thus, the phylogenetic relationships of the extinct tinamous proposed by the presented study are consistent with the palaeoenvironmental conditions inferred for the Neogene of southern South America, and the ecology of their closest living relatives.

ACKNOWLEDGEMENTS

We would especially like to thank Dan Ksepka for his early participation, helpful comments, and discussions on the anatomy of Palaeognathae. We also thank Marcos Mirande for general advice on phylogenetic analysis. E. Guanuco (Fundación Miguel Lillo) produced the illustrations. For permission to examine specimens under their care, we especially thank the curators and staff of the Museum für Naturkunde (Berlin, Germany), Zoological Museum University of Copenhagen (Copenhagen, Denmark), the Natural History Museum (London, UK), Museo Argentino de Ciencias Naturales (Buenos Aires, Argentina), Museo La Plata (La Plata, Argentina), Museu de História Natural de Taubaté (Sao Paulo, Brazil), Fundación Miguel Lillo (Tucumán, Argentina), American Museum of Natural History (New York, USA), Natural History Museum of Los Angeles County (Los Angeles, USA), National Museum of Natural History (Washington D.C., USA), Field Museum of Natural History (Chicago, USA), Museum of Comparative Zoology, Harvard University (Cambridge, USA), Museum of Natural Science, Louisiana State University (Baton Rouge, USA), Museum of Natural History, The University of Kansas

(Lawrence, USA), University of California, Museum of Vertebrate Zoology (Berkeley, USA), Museum of Zoology, University of Michigan (Ann Harbor, USA), and Yale Peabody Museum of Natural History (New Haven, USA). This project was supported by the Consejo Nacional de Investigaciones Científicas y Técnicas (CONICET, Argentina), Fundación Miguel Lillo (FML, Argentina), Collection Study Grants (Ornithology, American Museum of Natural History), and a Return Fellowship for Research Fellows (Alexander von Humboldt Foundation, Germany). Finally, we are indebted to Estelle Bourdon and an anonymous reviewer for comments that improved the article.

REFERENCES

Abello MA, Ortiz Jaureguizar E, Candela AM. 2012. Paleoecology of the Paucituberculata and Microbiotheria (Mammalia, Marsupialia) from the late Early Miocene of Patagonia. In: Vizcaíno SF, Kay RF, Bargo MS, eds. *Early Miocene paleobiology in Patagonia*. New York: Cambridge University Press, 156–173.

Alix HE. 1874. Memoireur l'osteologie et la myologie du *Nothura major*. *Journal of Zoolgie* **3:** 252–285.

Baumel JJ, King AS, Breazile JE, Evans HE, Vanden Berge JC. 1993. *Handbook of avian anatomy: nomina anatomica avium, 2th ed*. Cambridge, MA: Publications of the Nuttall Ornithological Club, 45–132.

Bertelli S. 2002. Filogenia del Orden Tinamiformes. Unpublished phD thesis, Universidad Nacional de Tucumán, Argentina.

Bertelli S, Chiappe LM. 2005. Earliest tinamous (Aves: Palaeognathae) from the Miocene of Argentina and their phylogenetic position. *Contributions in Science* **502:** 1–20.

Bertelli S, Giannini NP. 2013. On the use of intergumentary charactersin bird phylogeny: the case of *Tinamus osgoodi* (Palaeognathae: Tinamidae) and plumage character coding. *Acta Zoologica Lilloana* **57:** 57–71.

Bertelli S, Giannini NP, Goloboff PA. 2002. A Phylogeny of the tinamous (Aves: Palaeognathiformes) base on integumentary characters. *Systematic Biology* **51:** 959–979.

Bledsoe AH. 1988. A phylogenetic analysis of poscranial skeletal characters of the ratite birds. *Annals of Carnegie Museum* **57:** 73–93.

Bock WJ. 1963. The cranial evidence for ratite affinities. *Proceedings of the XIII International Ornithological Congress*, pp. 39–54.

von Boetticher H. 1934. Beitrag zu einem phylogenetisch begründeten, natürlichen System der Steißhühner (Tinami) auf Grund einiger taxonomisch verwertbarer Charaktere: mit einer Stammbaumskizze. *Jenaische Zeitschrift für Naturwissenschaft* **69:** 169–192.

Bourdon EA, Ricqlés DE, Cubo J. 2009. A new transantarctic relationship: morphological evidence for a Rheidae-Dromaiidae-Casuariidae clade (Aves, Palaeognathae, Ratitae). *Zoological Journal of the Linnean Society* **156:** 641–663.

Bown TM, Larriestra CM. 1990. Sedimentary paleoenvironments of fossil platyrrhine localities, Miocene Pinturas Formation, Santa Cruz Province, Argentina. *Journal of Human Evolution* **19:** 87–119.

Brea M, Zucol AF, Iglesias A. 2012. Fossil plant studies from the Early Miocene of the Santa Cruz Formation: paleoecology and paleoclimatology at the passive margin of Patagonia, Argentina. In: Vizcaíno SF, Kay RF, Bargo MS, eds. *Early Miocene paleobiology in Patagonia*. New York: Cambridge University Press, 104–129.

Brodkorb P. 1963. Catalogue of fossil birds. *Bulletin of Florida State Museum* **7:** 179–293.

Cabot J. 1992. Order Tinamiformes. In: del Hoyo J, Elliot A, Sargatal J, eds. *Handbook of the Birds of the World*, *Vol. 1*. Barcelona: Lynx Edicions, 112–138.

Campbell KE. 1979. The non-passerine Pleistocene avifauna of the Talara tarseeps, Northwestern Perú. *Royal Ontario Museum, Life Science Contributions* **118:** 1–203.

Chandler RM. 2012. A new species of tinamou (Aves: Tinamiformes, Tinamidae) from the Early-Middle Miocene of Argentina. *PalArch's Journal of Vertebrate Palaeontology* **9:** 1–8.

Chiappe LM. 1991. Fossil birds from the Miocene Pinturas Formation of southern Argentina. *Journal of Vertebrate Paleontology* **11:** 21–22.

Clarke JA. 2004. Morphology, phylogenetic taxonomy, and systematics of *Ichthyornis* and *Apatornis* (Avialae: Ornithurae). *Bulletin of the American Museum of Natural History* **286:** 1–179.

Cracraft J. 1974. Phylogeny and evolution of the ratites birds. *Ibis* **116:** 494–521.

Cracraft J. 1986. The origin and early diversification of birds. *Paleobiology* **12:** 383–399.

Dzerzhinskii FY. 1983. Chelustnoy apparat tinamou *Eudromia elegans.* K voprosu o morfobiologicheskoy spetsifike chelustnogo apparata paleognat. *Trudy Zoologicheskogo Instituta Akademii Nauk SSSR* **116:** 12–33.

Elzanowski A. 1987. Cranial and eyelid muscles and ligaments of the tinamous (Aves: Tinamiformes). *Zoologische Jahrbücher: Abteilung für Anatomie und Ontogenie der Tiere* **116:** 63–118.

Ericson PGP. 1997. Systematic relationships of the palaeogene family Presbionithidae (Aves: Anseriformes). *Zoological Journal of the Linnean Society* **121:** 429–483.

Ericson PGP, Anderson CL, Britton T, Elzanowski A, Johansson US, Källersjö M, Ohlson JI, Parsons TJ, Zuccon D, Mayr G. 2006. Diversification of Neoaves: integration of molecular sequence data and fossils. *Biology Letters* **2:** 543–547.

Fjeldså J, Krabbe N. 1990. *Birds of the high Andes*. Copenhagen: Zoological Museum Danmark.

Genise JF, Bown TM. 1994. New Miocene scarabeid and hymenopterous nests and early Miocene (Santacrucian) paleoenviroments, Patagonian Argentina. *Ichnos* **3:** 107–117.

George JC, Berger AJ. 1966. *Avian myology*. London: Academic Press.

Goloboff PA, Farris JS, Källersjö M, Oxelman B, Ramírez MJ, Szumik CA. 2003. Improvements to resampling measures of group support. *Cladistics* **19:** 324–332.

Goloboff PA, Farris JS, Nixon K. 2008a. TNT: tree analysis using new technology, vers. 1.1 (Willi Hennig Society Edition). Available at: http://www.zmuc.dk/public/phylogeny/tnt

Goloboff PA, Farris JS, Nixon K. 2008b. TNT, a free program for phylogenetic analysis. *Cladistics* **24:** 774–786.

Hackett SJ, Kimball RT, Reddy S, Bowie RCK, Braun EL, Braun MJ, Chojnowski JL, Cox WA, Han KL, Harshman J, Huddleston CJ, Marks BD, Miglia KJ, Moore WS, Sheldon FH, Steadman DW, Witt C, Yuri T. 2008. A phylogenomic study of birds reveals their evolutionary history. *Science* **320:** 1763–1768.

Haddrath O, Baker B. 2012. Multiple nuclear genes and retroposons support vicariance and dispersal of the palaeognaths, and an Early Cretaceous origin of modern birds. *Proceedings of the Royal Society of London B* **279:** 4617–4625.

Harshman J, Braun EL, Braun ML, Huddleston CJ, Bowie RCK, Chojnowski JL, Hackett SJ, Han KL, Kimball RT, Marks BD, Miglia KJ, Moore WS, Reddy S, Sheldon FH, Steadman DW, Steppan SJ, Witt CC, Yuri T. 2008. Phylogenomic evidence for multiple losses of flight in ratite birds. *Proceedings of the National Academy of Sciences of the United States of America* **105:** 13462–13467.

Houde PW. 1988. *Paleognathous birds from the early Tertiary of the northern Hemisphere*. Cambridge: Publications of Nutall Ornithology Club.

Hudson GE, Schreiweis DO, Wang SYC, Lancaster DA. 1972. A numerical study of the wing and leg muscles of tinamous (Tinamidae). *Northwest Science* **46:** 207–255.

Kay RF, Perry JMG, Malizak M, Allen KL, Kirk EC, Plavcan JM, Fleagle JG. 2012. Paleobiology of Santacrucian primates. In: Vizcaíno SF, Kay RF, Bargo MS, eds. *Early Miocene paleobiology in Patagonia*. New York: Cambridge University Press, 306–331.

Lakjer T. 1926. *Studien über die Trigeminus-versorgte Kaumuskulatur der Sauropsiden*. Kopenhagen: Reitzel.

Lee K, Feinstein J, Cracraft J. 1997. The phylogeny of ratite birds: resolving conflicts between molecular and morphological data sets. In: Mindell DP, ed. *Avian molecular evolution and systematics*. San Diego: Academic Press, 173–211.

Livezey BC. 1997. A phylogenetic classification of waterfowl (Aves, Anseriformes), including selected fossil species. *Annals of Carnegie Museum* **66:** 457–496.

Livezey BC, Zusi RL. 2007. Higher-order phylogeny of modern birds (Theropoda, Aves: Neornithes) based on comparative anatomy. II. Analysis and discussion. *Journal of the Linnean Society* **149:** 1–95.

Lucas FA. 1886. Notes on the osteology of the spotted tinamou (*Nothura maculosa*). *Proceedings of the United States National Museum* **11:** 157–158.

Maijer S. 1996. Distinctive song of highland form *maculicollis* of the red-winged tinamou (*Rhynchotus rufescens*): evidence for species rank. *Auk* **113:** 695–697.

Mayr G. 2011. On the osteology and phylogenetic affinities of *Morsoravis sedilis* (Aves) from the early Eocene Fur Formation of Denmark. *Bulletin of the Geological Society of Denmark* **59:** 23–35.

Mayr G, Clarke J. 2003. The deep divergences of neornithine birds: a phylogenetic analysis of morphological characters. *Cladistics* **19:** 527–553.

Mercerat A. 1897. Note sur les oisseaux fossiles de la République Argentine. *Anales de la Sociedad Científica Argentina* **43:** 222–240.

Miranda-Ribeiro A. 1937. Notas ornithológicas, Tinamidae. *Revista do Museo Paulista* **23:** 667–788.

Parker WK. 1866. On the osteology of gallinaceous birds and tinamous. *Transactions of the Zoological Society of London* **5:** 149–241.

Picasso MBJ, Degrange FJ. 2009. El género *Nothura* (Aves, Tinamidae) en el Pleistoceno (Formación Ensenada) de la provincia de Buenos Aires, Argentina. *Revista Mexicana de Ciencias Geológicas* **26:** 428–432.

Pol D, Escapa IH. 2009. Unstable taxa in cladistic analysis: identification and the assessment of relevant characters. *Cladistics* **25:** 515–527.

Porzecanski AL. 2003. Historical biogeography of the South American aridlands: a molecular study of endemic avian taxa. Unpublished D. Phil. Thesis, Columbia University, New York.

Pycraft WP. 1900. On the morphology and phylogeny of the Palaeognathae (Ratitae and Crypturi) and Neognathae (Carinatae). *Transactions of the Zoological Society of London* **15:** 149–290.

Saiff E. 1988. The anatomy of the middle ear of the Tinamiformes (Aves: Tinamidae). *Journal of Morphology* **196:** 107–116.

Salvadori T. 1895. *Catalogue of the Chenomorphae (Palamedeae, Phoenicopteri, Anseres), Crypturi and Ratitae in the Collection of the British Museum*. London: British Museum (Natural History).

Silveira LF, Höfling E. 2007. Osteologia craniana dos Tinamidae (Aves: Tinamiformes) com implicações sistemáticas. *Boletin da Museo Emílio Goeldi* **2:** 15–54.

Smith JV, Braun EL, Kimball RT. 2013. Ratite nonmonophyly: independent evidence from 40 novel loci. *Systematic Biology* **62:** 35–49.

Tambussi C. 1987. Catálogo crítico de los Tinamidae (Aves: Tinamiformes) fósiles de la República Argentina. *Ameghiniana* **24:** 241–244.

Tambussi C. 1989. Las aves del Plioceno-tardío Pleistoceno-temprano de la Provincia de Buenos Aires. Unpublished dissertation, Universidad Nacional de La Plata, Argentina.

Tambussi C, Noriega J. 1996. Summary of the Avian Fossil Record from Southern South América. *Münchner Geowissenschaftliche Abhandlungen* **30:** 245–264.

Tambussi C, Noriega J, Tonni EP. 1993. Late Cenozoic birds of Buenos Aires Province (Argentina): an attempt to document quantitative faunal changes. *Paleoecology* **101:** 117–129.

Tambussi C, Tonni EP. 1985. Un Tinamidae (Aves: Tinamiformes) del Mioceno tardío de La Pampa (República Argentina) y comentarios sobre los tinámidos fósiles argentinos. *Revista de la Asociación Paleontológica Argentina* **14:** 4.

Tejedor MF. 2002. Primate canines from the early Miocene Pinturas Formation, southern Argentina. *Journal of Human Evolution* **43:** 127–141.

Tonni EP. 1977. Los Tinámidos fósiles argentinos I. El género Tinamisornis Rovereto, 1914. *Ameghiniana* **14:** 225–232.

Verheyen R. 1960. Les Tinamous dans les systemes ornithologiques. *Bulletin de l'Institut Royal des Sciences Naturelles de Belgique* **36:** 1–11.

Vizcaíno SF, Kay RF, Bargo MS. 2012. A review of the paleoenviroment and paleoecology of the Miocene Santa Cruz Formation. In: Vizcaíno SF, Kay RF, Bargo MS, eds. *Early Miocene paleobiology in Patagonia*. New York: Cambridge University Press, 331–336.

Webb M. 1957. The Ontogeny of the cranial bones, cranial peropheral and cranial parasympathetic nerves, together with a study of the visceral msucles of *Struthio*. *Acta Zoologica* **38:** 81–203.

Worthy TH, Holdaway RN. 2002. *The lost world of the Moa*. Bloomington: Indiana University Press.

Worthy TH, Scofield RP. 2012. Twenty-first century advances in knowledge of the biology of moa (Aves: Dinornithiformes): a new morphological analysis and moa diagnoses revised. *New Zealand Journal of Zoology* **39:** 87–153.

APPENDIX 1

Data set used in the present analysis. Characters 12, 17, 19, 24, 34, 39, 42, 44, 47, 54, 57, 62, 69, 80, 92, 95, 99, 100, 101, 111, 115, and 116 were considered additive.

†*Ichthyornis dispar*	?????1????	0101?110??	????2?????	???????000	00--?000?1	????[12]0??01	0---00-010	0000102000
†*Lithornis* sp.	00?0111101	00010??210	0000000110	??01?11110	2210?0???2	0011?01001	0---000010	0000100000
Rhea americana	0011110210	100101020-	0001000110	1000011110	1110000120	??1?---000	0---11-100	------011-
Apteryx australis	00111-1201	00000--22-	-00020011-	0001210110	1200000011	??1?---000	0---11-100	------201-
Megapodius freycinet	00001010-0	0000[01]0000-	0-1-000000	0--000-001	30-0110031	??0?100201	1110000010	1000001101
Penelope superciliaris	00001010-0	000010000-	0-1-000000	0--000-002	30-0110031	1101000201	1110000010	0000000201
Gallus gallus	00001010-0	000000000-	0-1-000000	0--000-002	30-0110031	1101000221	1110000010	0000000201
Chauna torquata	00001000-0	000001000-	021-1?0001	0--000-001	30-0210031	??11202001	0---002010	0000101200
Anas flavirostris	00111000-0	000011000-	021-110001	0--020-000	30-0210030	0011200001	0---002010	0000101000
Mergus serrator	00011100-0	000011000-	021-110001	0--020-000	30-0210031	0011200001	0---002010	0000100000
Tinamus solitarius	1000010101	0120001110	0001?00010	0001010111	12010000[12]1	0011000210	1100000002	1100001000
Tinamus major	1000010101	0120001110	0001000010	0001010111	1201000011	0011000110	1100000002	1100001000
Tinamus tao	1000010101	0120001110	0001000010	0001010111	1201000011	0011000210	1100000002	1100001000
Tinamus guttatus	1000010101	012?001110	0001?00010	0001010111	1201000011	0011000110	1100000002	1100001000
Crypturellus tataupa	1000010101	0121001110	1101000010	000?011111	1200100101	0011110210	1010000002	1111012?01
Crypturellus parvirostris	1000010101	0121001110	1101000010	000?011111	1200100101	0011110210	1010000002	1111012?01
Crypturellus obsoletus	1000010101	0121001110	0101000010	0001010111	1200100101	0011110210	1010000002	1111011001
Crypturellus variegatus	1000010101	0121001110	0001000010	0001010111	120?000101	0011110210	1010000002	1111011001
Crypturellus erythropus	1000010101	0121001110	0001000010	0001010111	1201000101	0011110210	1010000002	1111011001
Crypturellus noctivagus	1000010101	0121001110	0001000010	0001010111	1201000101	0011110210	1010000002	1111011001
Crypturellus undulatus	1000010101	0121001110	?001000010	0001010111	120?000001	0011110210	1010000002	1111011001
Crypturellus soui	1000010101	0121001110	0001000010	0001010111	1200000001	0011110210	1010000?02	1111011?01
Crypturellus cinereus	1000010101	0121001110	0001000010	0001010111	1200000101	0011110210	1010000012	1111011001
Crypturellus boucardi	1000010101	0121001110	0001000010	0001010111	1200000001	0011110210	1010000012	1111011001
Crypturellus cinnamomeus	1000010101	0121001110	0001000010	0001010111	120?000011	0011?10210	1010000002	1111011001
Crypturellus barletti	1000010101	0121001110	0001000010	000?010111	1201000001	0011110210	1010000002	1111011001
Crypturellus transfaciatus	1000010101	0121001110	0001000010	0001010111	1201000011	0011110210	1010000?02	1111011001
Crypturellus brevirostris	1000010101	0121001110	0001000010	0001010111	1201000001	0011110?10	1010000002	1111011001
Nothura minor	1000000101	0001111110	0101000011	0020011111	1210100201	0011211220	111000001?	0000012000
Nothura boraquira	1000000101	0001111111	0101000011	0111011111	1210100201	0011201??0	1110000012	0000012?00
Nothura maculosa	100000[01]101	0001111111	1101000011	011[01]011111	1210100201	0011201[23]20	1110000012	0000012100
Nothura darwinii	1000001101	0001111111	1101000011	0111011111	1210100201	0011201220	111[01]001012	0000012100
Nothoprocta ornata	1100101211	0001011111	1001001011	1010112112	2210210201	1111201310	111000[01]012	0001012[01]00
Nothoprocta cinerascens	1[01]00101201	0011011111	0001001011	101[01]011111	1210200200	11112012[12]0	101000[01]0[01]2	0100012100
Nothoprocta pentlandii	1[01]001012[01]1	0001011111	1001001011	1010112112	2210210201	11112[01]1320	111[01]001012	0000012100
Nothoprocta perdicaria	1100101?21	0001?11111	1001001011	1010112112	221021020?	????201310	1110001012	0001012000
Nothoprocta taczanowskii	1111101201	0001011111	100120?011	1010112112	121021020?	????201320	1111001012	0000012100
Rhynchotus maculicollis	1111111211	0000011110	1001001010	001010-111	1220100211	1011201220	1111001012	000[01]012100
Rhynchotus rufescens	1111111211	0000011110	1001001010	001010-111	1220100201	10112012?0	1010001012	000[01]012[01]00
Eudromia elegans	1000001201	1010010112	0100000010	0111011111	0200001221	0001100230	11200000[01]2	1111012000
Eudromia formosa	1000000201	1010010112	010000001[01]	0111011111	0200001221	0001100230	1120000002	1111012000
Tinamotis pentlandi	1010000101	10?0010112	0100000111	0021011111	1201000110	0000100230	1120000002	0111012000
Tinamotis ingoufi	1000001101	1001010112	0100000111	0021011111	1201000110	0000100230	1120000002	0111012000
Tinamotis nanus	1000000101	0000111110	?101000010	0021011111	120010020?	????211220	111100?011	0000011000
Nothocercus bonapartei	1000010101	0010001110	0001110010	0001010111	120100001?	????110130	1111000012	0000000000
Nothocercus julius	1000010101	0010001110	0001110010	0001010111	120100001?	????110230	1111000012	0000000000
Nothocercus nigrocapillus	1000010101	00??001110	0?01110010	0001010111	1201000001?	????110?30	111?000012	0000000000
†*Eudromia olsoni*	??????????	??????????	??????????	??????????	??????????	??????????	???????0?2	11110??000
†*Nothura paludosa*	??????????	??????????	??????????	??????????	??????????	??????????	???????012	000001[12]100
†MACN-sc-1010	??????????	??????????	??????????	??????????	??????????	??????????	???????0?2	111100?0??
†MACN-sc-1013	??????????	??????????	??????????	??????????	??????????	??????????	???????0?2	101100?0??
†*Eudromia* sp.	??????????	??????????	??????????	??????????	??????????	??????????	???????0?2	?10101[12]0??
†*Crypturellus reai*	??????????	??????????	??????????	??????????	??????????	??????????	??????????	????????01
†MACN-sc-H	??????????	??????????	??????????	??????????	??????????	??????????	??????????	????????0?
†MACN-sc-T	??????????	??????????	??????????	??????????	??????????	??????????	??????????	??????????
†*Nothura* sp.	??????????	??????????	??????????	??????????	??????????	??????????	???????0?2	000101????

APPENDIX 1 *Continued*

†*Ichthyornis dispar*	20-0110001	01???2???0	0?001?0020	???003????	??????????	??????????	??????????	???????
†*Lithornis* sp.	1100000021	0?11021000	01??1?1010	011102????	??????????	??????????	??????????	???????
Rhea americana	-0-0-00?20	--0--10-01	0000-110-1	11?10200?0	????0?0???	????????0?	???????000	?0?????
Apteryx australis	-0-0-00020	--3--20-00	0300111[01]20	00100110-0	??????????	????????0?	???????000	?0-????
Megapodius freycinet	0100000000	0011000-00	0?00000110	03-10020?0	-????1???2?	??????????	???????000	?0??0??
Penelope superciliaris	0100000100	0010000-00	1200100110	03-1002020	-????1???2?	??????????	???????000	???????
Gallus gallus	0100000100	0020000-00	2201100110	03-1002???	??????????	??????????	??????????	???????
Chauna torquata	0100000011	0021000-00	2000000111	00-002?020	-????1???2?	??????????	???????000	???????
Anas flavirostris	0100000120	0010000-00	0?00010110	03-003?020	?????1???2?	??????????	???????000	???????
Mergus serrator	0100000120	0000000-00	00001?0110	03-003????	??????????	??????????	??????????	???????
Tinamus solitarius	1101110[01]10	1010021001	21?00011?1	0210031???	??????????	??????????	??????????	???????
Tinamus major	1101110010	1010021001	2100001100	0211021121	0121010121	1001000000	0100010112	1121101
Tinamus tao	1101110010	1010021001	2100001101	0210031???	??????????	??????????	??????????	???????
Tinamus guttatus	1101110010	1010021001	2100001101	0211031???	??????????	??????????	??????????	???????
Crypturellus tataupa	2101110000	1030021001	1300001111	0210021121	1110010120	1101000000	0100110112	1121101
Crypturellus parvirostris	2101110000	1030021001	1300001111	0210021121	1110010120	1101000000	0100110???	???????
Crypturellus obsoletus	2101110000	1030021001	1300001111	0210021121	1110010120	1101000000	0100110???	???????
Crypturellus variegatus	2101110000	1020021001	2300001111	0210021???	??????????	??????????	??????????	???????
Crypturellus erythropus	2101110?00	1020021001	2300001111	0210021121	1110010120	1101000000	0100110???	???????
Crypturellus noctivagus	2101110000	1020021001	2300001111	0210021???	??????????	??????????	??????????	???????
Crypturellus undulatus	2101110000	1020021001	2300001111	0210021???	??????????	??????????	??????????	???????
Crypturellus soui	2101110000	1020021001	1300001111	0210021121	1110010120	1101000000	0100110112	1121111
Crypturellus cinereus	2101110000	1030021001	1300001111	0210021???	??????????	??????????	??????????	???????
Crypturellus boucardi	2101110000	1020021001	1300001111	0210021???	??????????	??????????	???????112	1121111
Crypturellus cinnamomeus	2101110100	1020021001	1300001111	0210021121	1110010120	1101000000	0100110112	1121111
Crypturellus barletti	2101110?00	1020021001	1300001111	0210021???	??????????	??????????	??????????	???????
Crypturellus transfaciatus	2101110100	1020021001	1300001111	0210021121	1110010120	1101000000	0100110???	???????
Crypturellus brevirostris	2101110100	1020021001	1300001111	0210021???	??????????	??????????	??????????	???????
Nothura minor	2111110100	1131121102	1300101111	1210021???	??????????	??????????	??????????	???????
Nothura boraquira	2111110?00	1131121102	1300101111	1?10021???	??????????	??????????	??????????	???????
Nothura maculosa	2111110100	1131121102	1300101111	11100[23]1101	0130100001	1001000010	1000-01111	0110000
Nothura darwinii	2111110100	1131121102	1300101111	1110031101	0130100001	1001000010	1000-01111	0110000
Nothoprocta ornata	211111010?	1131121102	[12]301101111	11100[23]1111	00-0200011	0000011110	1000-02111	0110000
Nothoprocta cinerascens	2111110100	1131121102	1301101111	1110031111	00-0200010	0000011110	1000002111	0110000
Nothoprocta pentlandii	2111110100	1131121102	1301101111	1110031111	00-0200011	0000011110	1000-02111	0110000
Nothoprocta perdicaria	2111110100	1131121102	1301101111	11100[23]1111	00-0200011	0000011110	1000-02111	0110000
Nothoprocta taczanowskii	2111110100	1131121102	1301101111	1110031???	??????????	??????????	??????????	???????
Rhynchotus maculicollis	2111110100	1131121102	1301001111	1110031111	0100200011	0000011110	0000-01???	???????
Rhynchotus rufescens	21[01]1110100	1131121102	?201001111	1110031111	0100200011	0000011110	0000-01???	???????
Eudromia elegans	2101100010	1020021001	2310011111	1000020101	0131201100	0010111011	0111000111	1110001
Eudromia formosa	21011[01]0010	1020021001	2310011111	10000[23]0101	0131201100	0010111011	0111000???	???????
Tinamotis pentlandi	2100101011	1020021011	2311111121	1110110101	00-0201100	0010011011	0111-00111	0100001
Tinamotis ingoufi	21001[01]1011	1020021011	2310111111	1110110???	??????????	??????????	??????????	???????
Tinamotis nanus	20-1000120	1131121102	1300101111	1?10021???	??????????	??????????	??????????	???????
Nothocercus bonapartei	11011[01]0100	[01]020121001	1200001l?0	0211031?2?	??????????	??????????	??????????	???????
Nothocercus julius	1101110100	0020121001	1200001110	0211031?2?	??????????	??????????	??????????	???????
Nothocercus nigrocapillus	1101110100	?020121001	1200001110	0211031?2?	??????????	??????????	??????????	???????
†*Eudromia olsoni*	210???????	??????????	??1??1????	??????????	??????????	??????????	??????????	???????
†*Nothura paludosa*	2111110000	11?????????	130010?111	1110021???	??????????	??????????	??????????	???????
†MACN-sc-1010	??????????	??????????	??????????	??????????	??????????	??????????	??????????	???????
†MACN-sc-1013	??????????	??????????	??????????	??????????	??????????	??????????	??????????	???????
†*Eudromia* sp.	??????????	??????????	??????????	??????????	??????????	??????????	??????????	???????
†*Crypturellus reai*	210111?0??	??????????	??????????	??????????	??????????	??????????	??????????	???????
†MACN-sc-H	???111100??	??????????	??????????	??????????	??????????	??????????	??????????	???????
†MACN-sc-T	??????????	??????????	????1?111?	??????????	??????????	??????????	??????????	???????
†*Nothura* sp.	??????????	??????????	??????????	??????????	??????????	??????????	??????????	???????

APPENDIX 2

List of morphological characters used in the cladistic analysis. Characters for which states could be arranged in a linear transformation series were coded as additive (non-additive and additive characters are indicated by '–' and '+', respectively).

0. – Os supraoccipitale, position of foramen v. occipitalis externa relative to the prominentia cerebellaris (Fig. 3): ventral of the prominentia (0); dorsal, proximal of the crista nuchalis transversa (1).
1. – Os supraoccipitale, development of sulcus v. occipitalis externa (Fig. 3): short grooves (0); ventrally extended and curved grooves (1). Ventrally extended and curved grooves were observed in *Rhynchotus* and *Nothoprocta*.
2. – Os supraoccipitale, crista nuchalis sagittalis (Fig. 3): absent (0); present (1). The area of the prominentia cerebellaris of tinamous is typically smooth (not marked by a crista nuchalis sagittalis), with the exception of *Rhynchotus*, *Tinamotis pentlandii*, and *Nothoprocta taczanowskii*, in which its surface is scarred by a marked crest.
3. – Os exoccipitale, processus paroccipitalis (Fig. 3): not developed, flat or poorly developed as a wing-like projection, approaching but not extending below the ventral margin of the otic cavity (0); distinctly prominent, projecting ventrally (1). A poorly developed processus paroccipitalis is found in some out-group taxa (Galliformes) and in all tinamous (except for *Rhynchotus* and *Nothoprocta taczanowskii*). Only this tinamou species posses a markedly prominent processus paroccipitalis; a similar condition is also present in other out-group taxa (e.g. Ratitae).
4. – Os exoccipitale, foramen n. vagi, nearer to the foramen n. ophthalmici than to foramen n. hypoglossum (Figs 3 and 5): no (0); yes (1).
5. + Fossa temporalis (Fig. 4): small temporal notch, smaller than otic cavity, not extending caudally beyond the cotyla quadratica squamosi (0); larger or about the same size as the otic cavity, caudal extension about or beyond the position of the cotyla (1). A well-developed fossa temporalis in Tinamidae (condition 1) and related Palaeognathae was described by Pycraft (1900); however, we observed variation in the development of this fossa among tinamous, for example, a distinct small temporal notch enclosed by a rostroventrally orientated processus zygomaticus together with a pointed processus postorbitalis characterizes the skull of the open area tinamous (with the exception of *Rhynchotus*) and some out-group taxa. We consider the highly derived skull morphology of *Apteryx* to be non-comparable for this character.
6. – Os squamosum, prominentia suprameatica (Elzanowski, 1987) developed as a distinct crest (Fig. 4): absent (0); present (1). The prominentia suprameatica flares out from the base of the processus zygomaticus, dorsal of the otic cavity (Elzanowski, 1987). Although this structure is absent or minimally developed in most tinamous, it projects as a wing-like crest in some open area taxa such as *Nothura*, *Nothoprocta*, and *Rhynchotus*, among others. In these taxa, the suprameatic prominence is clearly visible both in lateral and ventral view.
7. – Os squamosum, processus zygomaticus (Fig. 4): absent or vestigial (0); present, variably developed (1); present, laterally compressed (2). The body of the processus zygomaticus in *Rhynchotus* and *Nothoprocta* (also in *Eudromia*, although less developed) is short and laterally compressed, projecting as a crest, which has been tentatively indentified as the area of attachment of the aponeurosis zygomatica (Elzanowski, 1987). This process is also distinctly compressed in the ratites (e.g. *Rhea* and *Apteryx*). A lower ridge is also distinguishable on the processus zygomaticus of other open-area tinamous. See character 33 of Mayr (2011) for conditions in out-group taxa.
8. – Os squamosum, ventral margin of the processus zygomaticus (Fig. 4): straight (0); notched (1). The notched margin of the proc. zygomaticus forms a border with the ala parasphenoidalis, roofing the otic cavity in Rheidae, *Rhynchotus*, and some species of *Nothoprocta* (e.g. *N. ornata*). A non-comparable state was assigned to Galloanseres (the process is absent or vestigial in these taxa, see character 7).
9. – Sutura frontoparietalis (Figs 3 and 4): absent (0); present (1) (Mayr, 2011: character 32).
10. – Os frontale, dorsal surface, distinct fossa at midline (Fig. 3): absent (0); present (1). The interorbital surface of the skull of most taxa is essentially flat; only in *Rhea*, *Eudromia*, and *Tinamotis* is it scarred by a rounded depression at midline. This condition differs from that of some Anseriformes, where the depression is a longitudinal concavity on the frontal region of the skull (depressio frontalis of Baumel *et al*., 1993).
11. – Orbita, margo supraorbitalis, glandular depressions (fossae glandularum nasales, Fig. 3): absent (0); present (1). The portion of the frontal bordering the orbit forms a sharp supraorbital margin in most tinamous; only in *Tinamus* and *Crypturellus* glandular depressions (i.e. fossae glandularum nasales) are developed on the dorsal supraorbital border; these depressions are shallow and narrow, bounded laterally by the ossicula supraorbitales, and separated by a wide space

(they do not reach the midline as in other birds, such as Charadriiformes, Procellariiformes, and others).

12. + Orbita, ossicula supraorbitales (Fig. 3): absent (0); incomplete row of ossicles (1); paired complete row, forming a robust supraorbital layer surrounding the fossae glandularum nasales (2). After Bertelli and Chiappe (2005, character 7). Parker (1866) described these ossicles forming a rough layer on the dorsal surface of the skull in Tinamidae, and Lucas (1866) noted their absence in *Nothura maculosa*; variation of these structures within Tinamidae was also mentionated by Elzanowski (1987). In *Tinamus* and *Crypturellus*, these ossicula enclose the fossae glandularum nasales on the margo supraorbitalis (character 11), whereas other species (e.g *Eudromia*, *Nothocercus*, and *Nothoprocta*) with ossicles in this area lack such depressions. Remains of supraorbital ossicles were observed in specimens of *Nothocercus bonapartei* and *Nothocercus julius*; owing to the preservation of the examined specimens, it was not possible to confirm a positive scoring for *Nothocercus nigrocapillus*. Based on the morphology of the irregular supraorbital margin observed in some specimens of *Tinamotis pentlandii*, it is likely that the ossicula were present in this species and lost after preparation; however, remains of these structures were not preserved in the examined specimens, and thus this taxon was coded as unknown '?'.
13. – Orbita, interorbital area (os frontale), dorsal surface (Fig. 3): broader than or of similar width as the internarial area (0); narrower (1). This character describes the variation observed in the width of the interorbital area of tinamous. The interorbital surface (excluding the fossae glandularum nasales) is wider than or subequal to the internarial area (at the caudal end of the external nares) in some tinamous (e.g. *Eudromia*, *Taoniscus*, and *Rhynchotus*), whereas it is distinctly narrower in *Nothura*, *Crypturellus*, and *Nothoprocta*, among others.
14. – Orbita, fonticuli orbitocraniales (Fig. 4): vestigial or absent (0); present, large foramina present (1). Only the open area taxa *Taoniscus* and *Nothura* present these rounded openings in the caudal wall of the orbita. Because of the highly modified nature of the skull in *Apteryx*, we consider the character non-comparable for this taxon.
15. – Orbita, sulcus, and foramen n. olfactorii forming a wide transversal fenestra, which perforates the septum interorbitale (Fig. 4): yes (0) no (1). Next to the dorsal margin of the septum interorbitale, the sulcus for the olfactory nerve and the ethmoid artery (i.e. sulcus n. olfactorii; Baumel and Witmer, 1993) is developed as a shallow and thin groove in the open-area tinamous; the foramen n. olfactorii is relatively smaller in *Eudromia* and *Tinamotis* than in other open-area groups. By contrast, both foramen and sulcus are greatly excavated in the forest taxa *Nothocercus*, *Tinamus*, and *Crypturellus*. We consider this character to be non-comparable in *Apteryx*, where this region of the skull is obscured by the highly modified orbital area.
16. – Orbita, septum interorbitale extensively ossified (Fig. 4): yes (0); no (1). After Bertelli and Chiappe (2005: character 1). The fonticuli interorbitales are typically present in most tinamous (only absent in *Tinamotis* and *Eudromia*).
17. + Os mesethmoidale (Fig. 4): does not reach rostrally beyond nasal–frontal hinge (0); extends rostrally immediately beyond the nasal–frontal hinge (1); extends far rostrally (2). Pycraft (1900: 198) discussed this feature and noted that the rostral extension in *Struthio* and *Rhea* exceeded that of other ratites. This feature was coded by Mayr (2011), albeit only with two states, recognizing the derived one in *Apteryx* and Rheidae. Cracraft (1986: character 50) reported the absence of a 'largely ossified' septum in the nasal region (mesethmoid) of Tinamidae, whereas Mayr (2011: character 8) noted the absence of this feature in both Tinamidae and Rheidae. In *Ichthyornis* this character has been inferred from the morphology of the praemaxilla (Clarke, 2004).
18. – Os ectethmoidale (Fig. 4): separated from os lacrimale (0); contacting or fused to os lacrimale, forming a lacrimal–ectetmoid complex (Cracraft, 1968) (1); extensively fused with os lacrimale and nasal capsule (2). After Bertelli and Chiappe (2005, character 5). Ericson (1997: character 6) coded the contact between these bones as present in Rheidae; we find this contact to be absent in all *Rhea* specimens examined (for a discussion of this character, see Cracraft, 1968: 330). Because these bones form part of the highly modified praeorbital region in *Apteryx*, we assigned an additional state (2) for this taxon.
19. + Lacrimal–ectethmoid complex (Fig. 4): narrow plate on ventromedial part of the antorbital wall, enclosing a wide and circular opening (foramen orbitonasale laterale) (0); wide plate that covers most of the antorbital wall (foramen orbitonasale laterale narrow (2); plate and enclosed foramen with triangular outline (1). Bertelli and Chiappe (2005, character 6) observed variation in the degree of development of the lacrimal–ectethmoid complex within Tinamidae. A narrow plate, enclosing a

circular foramen orbitonasale laterale characterizes the antorbital area of the skull of the forest tinamous). Among the open-area groups, this condition is only present in *Rhynchotus*, *Taoniscus*, and the species *Nothura minor*. A non-comparable state was assigned to out-group taxa in which the lacrimal–ectethmoid complex is absent (character 18).

20. – Os lacrimale, dorsal surface of the head (Fig. 3): expanded (0); very narrow (1). In tinamous, the lacrimal contacts the frontal and nasal; this condition is similar in *Apteryx* and Galliformes; by contrast, in *Rhea* and Anhimidae it articulates only with the nasal (Cracraft, 1968). The development of the dorsal surface of the lacrimals varies across species in tinamous. Only in the open-area tinamous *Rhynchotus*, *Taoniscus*, *Nothura darwinii*, *Nothura maculosa*, and most species of *Nothoprocta* (except *Nothoprocta cinerascens*) are the lacrimals distinctively narrower than in any other tinamous or out-group taxa (state 1). This character was scored as non-applicable for *Apteryx*, the lacrimals of which are not exposed on the dorsal surface of the skull. In *Rhea* this condition was scored as expanded (0), because the main body of the lacrimal is dorsally wide, regardless of the presence of a supraorbital process projecting caudolaterally.
21. – Os lacrimale, lacrimal duct (Fig. 4): perforating the lacrimal as a foramen or almost complete foramen (0); forming a wide notch (incisura ductus lacrimalis) (1); not perforating the lacrimal (2). Because its delicate nature makes it prone to damage, this character could not be confirmed in some taxa (e.g. *Crypturellus* and *Nothocercus*) with partially broken lacrimals. The incisura ductus lacrimalis (1) was coded as present if the lacrimal notch was distinctly wide dorsoventrally, forming a slender pediculus lacrimalis (Elzanowski, 1987). This character was scored as non-applicable in Galliformes, in which the ventral projection of the lacrimal in front of the orbit is absent.
22. – Os parasphenoidale, processus basipterygoideus, developed as a large and ovoid facet for articulation with the pterygoid (Mayr 2011: character 24; Fig. 5): no (0), yes (1).
23. – Os parasphenoidale, processus basipterygoideus (Fig. 5): stout process (0); elongated (1). The presence of a slender processus basipterygoideus is the most widely distributed condition within tinamous. Because of morphological differences (character 22), we coded this character as non-comparable for Galloanseres.
24. + Os parasphenoidale, processus parasphenoidalis medialis, aspect in caudal view (Fig. 3): absent (0); weakly developed ventrally as a low bump (1); prominent, developed as a conspicuous bony knob (2). Mayr (2011; character 30) distinguished only two states for this character. Within tinamous, these processes are prominent only in *Nothoprocta taczanowskii*, and are poorly developed in *Nothocercus*. Processus mediales parasphenoidales of the lamina parasphenoidalis are equivalent to the 'mamillary processes' of Pycraft (1900), the 'basal tubercles of the basitemporal plate' of Lee *et al*. (1997), as well as to 'medial processes of the parashenoid' (Bock, 1963).
25. – Os parasphenoidale, lamina parasphenoidalis (basitemporal plataform), medial crest marked: absent (0); present (1). A distinct medial ridge was observed on the rostral end of the basitemporal plataform of *Nothocercus* specimens.
26. – Os parasphenoidale, lamina parasphenoidalis, bony lateral projection directly rostral of ostium canalis carotici (Fig. 5): absent (0); present (1). These short and pointed processes, projecting towards the processus basipterygoideus, only occur in *Rhynchotus* and most *Nothoprocta* species.
27. – Os parasphenoidale, ostium canalis carotici more caudally placed, at about the middle of the lamina parasphenoidalis (Fig. 5): no (0); yes (1). Condition 1 is only found in *Tinamotis* within Tinamidae; in all other tinamous the ostium opens on each side of the lamina parasphenoidalis, close to the eustachian tube openings.
28. – Tuba auditiva (Fig. 5): open rostral, close to midline (0); open laterally, widely separated (1). In all palaeognaths these rostral openings are widely separated (Mayr, 2011: character 29).
29. – Os palatinum, rostrocaudally wide pars choanalis (Fig. 5): present (0); absent (1). Within Tinamidae, the pars choanalis of most open-area groups (except for *Rhynchotus*) is somewhat narrow rostrocaudally, with a well-developed processus caudomedialis. This condition differs from other tinamous, with a wider pars lateralis and a small or vestigial processus caudomedialis. Although this projection is variable within Lithornithidae, it is vestigial in *Lithornis* (Houde, 1988, p. 20). Codings for *Taoniscus nanus* were based on data from Silveira and Höfling (2007). We consider this character to be non-comparable for *Apteryx*.
30. – Os palatinum, processus maxillaris (Fig. 5): gradually curved from pars choanalis, facing obliquely ventromedially (0); contact distinctly curved, processes facing ventrally (1). This condition is typical of the species of *Nothoprocta*. Codings for *Taoniscus nanus* were based on data from Silveira and Höfling (2007).

31. Os palatinum, jugamentum maxillopalatinum (Elzanowski, 1987): absent (0); present (1). A distinct medial wing-like projection (jugamentum maxillopalatinum of Elzanowski, 1987) is present in the open-area groups *Nothura* and *Eudromia*. For an assessment of homologous conditions (e.g. processus maxillopalatini fused along midline), we considered out-group taxa non-comparable for this character.
32. – Processus maxillares of the ossa palatina and processus maxillopalatini of the ossa maxillaria (Fig. 5): mediolaterally wide plates (wider than fossa choanalis) (0); mediolaterally narrow plates (same width or narrower than fossae) (1); distinctly narrower than fossae, the latter with rounded proximal end (2). The processus maxillares of the ossa palatina and the processus maxillopalatini of the ossa maxillaria form slender plates or are slightly constricted mediolaterally (enclosing wide fossae choanalis) in most open-area tinamous (states 1 and 2), whereas these processes are wide throughout nearly their length (with narrow fossae) in the forest groups (state 0). Codings for *Taoniscus nanus* were based on data from Silveira and Höfling (2007). We consider Galloanseres non-comparable for this character (see character 31).
33. – Os quadratojugale, dorsal process (Fig. 4): absent or vestigial (0), present (1). A pointed process on the dorsal surface of the os quadratojugale is present in Tinamidae (except for *Nothoprocta* and *Rhynchotus*).
34. + Maxilla, rostrum maxillare, length with respect to the craniocaudal length of the external nares in lateral view (Figs 3 and 4): shorter (0); equal or longer (1); distinctly longer (2).
35. – Maxilla and mandibula, rostrum maxillare (upper mandible) and rostrum mandibularis (lower mandible), dorsal and ventral plate, lateral grooves: absent (0); present (1) (Mayr, 2011: character 40; Bertelli *et al*. 2002; Bertelli and Giannini, 2013). This character was modified from Bertelli *et al*. (2002: characters 1 and 4, which are correlated). These grooves, and their counterparts in the mandible, correspond to the unique tripartite rhamphothecal structure of palaeognaths. This character was considered non-comparable for Galloanseres (lateral grooves absent, character 35).
36. – Mandibula, rostrum mandibulare, ventral surface, lateral grooves: caudally convergent and contacting each other (0); parallel (1); caudally divergent (2). Character 3 of Bertelli *et al*. (2002).
37. – Mandibula, rostrum mandibulare, dorsal surface: symphysis concave (0); symphysis flat (1) (Mayr, 2011; character 43).
38. – Mandibula, dentary: unforked in lateral view, or with weakly developed dorsal ramus (0); strongly forked, having well-developed dorsal rami (1) (Mayr, 2011).
39. + Mandibula, ramus mandibularis (Fig. 4): straight (0); only slightly decurved or decurved towards tip (1); markedly decurved (2). Modified from Bertelli *et al*. (2002) and Bertelli and Giannini (2013).
40. – Mandibula, processus retroarticularis (Fig. 6): absent (0); poorly projected, as a small and rounded tubercle (1); distinctly projected, as a short and stout process (2); long and compressed blade-like process, strongly projected (3). Most tinamous (except for *Eudromia*) exhibit a small retroarticular process (state 1). This condition was also described for tinamous by Parker (1866) and *Rhea* by Pycraft (1900). The presence of a long and compressed retroarticular process is a synapomorphy of Galloanseres (Cracraft, 1988; Mayr, 2011), and was coded as a separated character state.
41. – Mandibula, cotyla caudalis and lateralis: separated (0); confluent (1; Fig. 6A).
42. + Mandibula, cotyla lateralis and caudalis (Fig. 6): short, kidney-shaped articular surface (0); elongate (1); long and strongly curved (2). Bock (1963) discussed the presence, absence, and homology of the cotyla lateralis and caudalis across a wide sampling of birds. Both cotylae are confluent in tinamous, *Lithornis* and *Apteryx*. Parker (1864) described the kidney-shaped condition in Tinamidae. We observed more variation in the degree of development of this cotyla among the specimens, and discriminate two additional character states. This character was considered non-applicable in taxa without cotyla caudalis; it is absent in *Ichthyornis* (Clarke, 2004).
43. – Mandibula, processus medialis mandibularis, facies articularis parasphenoidalis (Fig. 6): vestigial or not developed (0); distinct (1). A medial facet, near the tip of the processus medialis mandibularis, is well developed in most forest tinamous (e.g. *Tinamus*, *Nothocercus*, and some *Crypturellus*) and *Tinamotis*, usually connected to the cotylae caudalis and lateralis, forming a common articular surface. The shape and position of these articular surfaces correlates with a process present in the lateral area of the lamina parasphenoidalis that articulates with the facet of the mandible (Baumel and Witmer, 1993).
44. + Mandibula, cotyla medialis (Fig. 6): shallow and somewhat round facet (0); distinct facet, extending to the medial border of the articular surface of the articular mandible (1); deep and craniocaudally elongated facet, protruding the medial border of the mandible (2). The cotyla

medialis is typically well developed in the species of *Nothoprocta*.

45. – Mandibula, processus medialis mandibularis, aspect in dorsal view (Mayr 2011: character 45; Fig. 6): triangular (0); long and narrow (1). Previously this character was considered together with character 42 as a single character (Bertelli and Chiappe, 2005). After further study, we observed that the shape of the processus medialis mandibularis and the development of cotylae caudalis et lateralis varies independently across the tinamou species examined; thus we opted to add an additional character to accommodate this morphological variation observed within Tinamidae. According to Bock (1963), the shape of the processus medialis mandibularis is correlated with the development of both m. depressor mandibulae and m. pterygoideus, which attach to this process. The outline of this process is generally triangular in Tinamidae, with the exception of the narrow and dorsally oriented process present in *Nothoprocta* (except for *Nothoprocta cinerascens*).
46. – Quadratum, processus mandibularis medialis, medial area (between articular condylae) in ventral view with a swollen aspect, inflated (Figs 5A and 6I): absent (0); present (1). Among tinamous, this condition is typical of *Eudromia*.
47. + Quadratum, processus mandibularis, prominentia submeatica of Elzanowski (1987; Fig. 6), dorsal projection in lateral view: absent or slightly developed (0); dorsally projected relative to the edge of the processus orbitalis (1); markedly more projected than the processus, with a marked ridge (2). Elzanowski (1987) named the dorsal projection of the processus mandibularis of the quadrate of tinamous prominentia submeatica.
48. – Quadratum, shape of the processus orbitalis (Fig. 6): curved and flaring out at its tip (0); almost straight, distal expansion less developed or absent, subequal in proportion with the rest of the process (1); wide and robust, distal expansion vestigial (2); wide at its base, with pointed tip (3). In most tinamous, the orbital process becomes flared and widens at its tip, and is generally elongated as opposed to the robust aspect of *Eudromia*. A robust processus orbitalis is also present in *Rhea*.
49. – Axis, corpus with pneumatic foramina on lateral sides (Fig. 7): no (0), yes (1). Mayr (2011: character 48).
50. – Axis, processus spinosus (Fig. 7): blunt processes (0), bladelike and curved (1).
51. – Axis, processus ventralis, distinct bladelike and curved projection (Fig. 7): absent (0); present (1).
52. – Axis, processus costalis (Fig. 7): absent or vestigial (0); present, well developed (1). Mayr (2011: character 50).
53. – First series of vertebrae cervicales (from third vertebra cervicalis), processus costales (Fig. 7): absent or poorly projected (0), well developed (1).
54. + Synsacrum, aspect of centrum and processus costales in ventral view (Fig. 10): centrum with a flat aspect and wide processus costales, not completely fused to the lamina (0); most vertebrae with compressed centrum; relatively narrow processes, fused to the lamina; caudal, most elements with morphology similar to condition 0 (1); vertebrae with compressed centrum; relatively narrow processus, fused to the lamina, processus costales gradually shorter towards caudal end of synsacrum (or caudal most absent, angular aspect of the caudal end of synsacrum) (2). Between 15 and 18 vertebrae comprise the synsacrum of tinamous (Parker, 1866; Verheyen, 1960); this character is related to the degree of fusion of the vertebrae synsacrales of the postacetabular portion of the synsacrum. State 2 is typical of open-area tinamous (except for *Eudromia* and *Tinamotis*), whereas the opposite condition is characteristic of *Tinamus* (state 0) and the galliform out-group taxa. Ratites were scored as not comparable because the strong lateral compression of the postacetabular portion of the synsacrum and ilia prevent the determination of character states.
55. – Synsacrum (vertebrae lumbicales), vertebral arches, dorsal swell of praeacetabular portion adjacent to the medial confluence of ilia (Fig. 10): absent (0); present (1). *Rhea* and *Apteryx* were scored as not comparable because the strong lateral compression of the praeacetabular portion of the ilia, which covers the vertebral arches of the synsacrum dorsally, prevents the determination of character states.
56. – Synsacrum, dorsal surface of postacetabular area, distinctly depressed (Fig. 10): absent (0); present (1); with marked muscular impressions (2). The dorsal area of the synsacrum of the open area tinamou (except for *Eudromia* and *Tinamotis*) is distinctly depressed (state 1); this morphology (which may represent the attachment areas of muscles of the tail, musculi levatores caudae) differs from that of some out-group taxa (e.g. *Chauna*), with two conspicuous muscular impressions, and thus it was coded as a separate condition (state 2).
57. + Thoracic vertebrae, fusion (Fig. 7): all unfused, notarium absent (0); three vertebrae fused (1); four vertebrae fused (2); five vertebrae fused (3).

After Bertelli and Chiappe (2005: character 11). A notarium composed of four fused thoracic vertebrae is the condition widely distributed within Tinamidae. Variation was observed in some species, such as of the genus *Nothocercus* (e.g. *Nothocercus bonapartei*) with three vertebrae fused, and most species of *Nothoprocta* (except *Nothocercus cinerascens*) with five thoracic vertebrae fused.

58. – Sternum, processus craniolateralis, dorsal view (Fig. 8): short, widely spaced (0); variably developed, craniolaterally orientated, less projected than the spina interna (1); greatly elongated cranially, more projected (or reaching) the spina interna (2); projecting laterally (3). This character describes the variation in the relative length and orientation of these processes. These processes are typically elongated in most open-area tinamous (except for *Eudromia* and *Tinamotis*). By contrast, the processus craniolaterales are distinctly short and widely separated in most out-group taxa, a condition that was scored as a separate state (0).
59. – Sternum, rostrum, spina externa: absent (0); present (1) (Livezey, 1997: character 60). The external spine is present in *Ichthyornis* (Clarke, 2004), although not blade-like (see Mayr 2011, character 70). This process is present in *Lithornis* (Houde, 1988: fig. 10). Livezey (1997) coded the external spine present in Tinamidae, but the feature is absent in tinamous (see also Bertelli 2002: character 117).
60. – Sternum, rostrum, spina interna (Fig. 8): absent (0); present (1). Lee *et al*. (1997: character 7) proposed the absence of a 'sternal manubrium' as a synapomorphy of ratites; the absence of this structure in ratites and its presence in Tinamidae was described by Parker (1866) and Pycraft (1900: 216); however, because this manubrium can comprise the external spine (*Chauna*, *Lithornis*, and *Ichthyornis*), the internal spine (Tinamidae), or both (Galliformes), we follow Bertelli (2002: characters 117 and 118) in recognizing separate characters. According to Baumel (1993), the spina externa is most often present in the sternal rostrum of birds. One notable exception to this trend are the Tinamidae, where the rostrum comprises just the internal spine (Pycraft, 1900: p. 221; Bertelli, 2002).
61. – Sternum, rostrum, relative width of spina interna rostri: slender, rostral end narrower than craniolateral process (0); wide, broader than craniolateral process (1). The width of the internal spine was measured at the cranial portion of this process. Within tinamous, the spina interna is narrow only in the genus *Crypturellus* and a few other species (e.g. *Nothoprocta cinerascens*). With the exception of Galliformes, this character was scored as not comparable for the out-group because these taxa lack an internal spine (character 59).
62. + Sternum, cranial projection of the spina interna rostri (Fig. 8): markedly elongate, markedly protruding cranially (0); variably developed (1); significantly short, measuring less than half of the length of the processus craniolateralis (2). In *Eudromia* and *Tinamotis* this process is particularly short; by contrast, it is clearly elongate in *Tinamus*. Out-group taxa without spina interna rostri were coded as non-comparable for this character.
63. – Sternum, spina interna in ventral view, strongly concave cranial edge (Fig. 8): absent (0); present (1). *Taoniscus nanus* and some species of the genus *Nothoprocta*, *Nothocercus*, and *Rhynchotus* show a characteristic spina interna with a deeply concave cranial border, and have been tentatively identified as the area of attachment for the membrana sternocoracoclavicularis (Baumel *et al*., 1993).
64. – Sternum, carina: absent (0); present (1). Cracraft (1974: 503) suggested the loss of this keel to be derived within Neornithes.
65. – Clavicles fused to form a furcula (Fig. 8): absent (0); present (1). The furcula in *Lithornis* and in most Tinamidae is U-shaped (Bertelli, 2002).
66. – Furcula (Fig. 8): robust and thick sternal end (0); weak and thin sternal end (1). The sternal end of some species of *Nothoprocta* and *Rhynchotus* is distinctly thinner than the scapular portion (state 1), as opposed to a robust condition as in most tinamous. A robust, U-shaped furcula has been described for tinamous by Parker (1866). This character was scored as non-comparable for out-group taxa without a furcula. In Galliformes this condition was coded as robust (0) because the sternal end of the furcula is thick, irrespective of the presence of a median apophysis (hypocleideum).
67. – Scapula (Fig. 8): separated from coracoid (0); fused to coracoid (1). Mayr (2011: character 68) coded the presence or absence of scapulocoracoid fusion.
68. – Scapula, caudal half of blade (Fig. 8): expanding distally, with a blunt club-like extremity (0); distal expansion reduced, generally broadest at midline and tapering distally (1). After Bertelli and Chiappe (2005: character 16). The scapula of the fossil tinamou *Nothura parvula* is almost completely preserved, with approximately the same width throughout its length, thus we suggest the scoring for this character as 1.

69. + Coracoid, omal end, dorsal foramen below cotyla scapularis (Fig. 9): not excavated (0); vestigial, poorly developed (1); well developed, large opening (2). After Bertelli and Chiappe (2005: character 18). Mayr and Clarke (2003) were uncertain about whether this structure was homologous to the supracoracoid nerve foramen, a structure that channels the n. supracoracoideus through the body of the coracoid, in some birds. Nonetheless, because the supracoracoid nerve foramen needs to pass through the coracoid for this nerve to innervate the m. supracoracoideus (Baumel, 1993) and the opening described by the present character does not traverse the entire body of the bone, these two structures cannot be homologous. Within tinamous, this foramen is most likely to be homologous (does not traverse the body of the coracoid), and it is a well-developed opening, except in *Taoniscus nanus*, which show an almost vestigial foramen. This foramen is visible in the coracoid of the fossil tinamous MACN-SC-10, MACN-SC-13, *Nothura parvula, Eudromia olsoni, Nothura* sp. and *Eudromia* sp., and therefore these taxa were scored as 2.
70. – Coracoid, shape of the facies articularis clavicularis in medial view (Fig. 9): circular to ovate (0); crescent shaped, with overhanging tuberculum brachiale protruding ventromedially (1). After Bertelli and Chiappe (2005: character 19). This character occurs in *Tinamus*, *Crypturellus*, and *Eudromia*. Ratites were scored as non-comparable (and following characters 70–74) because both scapula and coracoid are fused, obscuring the morphology of the proximal end of the coracoid. *Eudromia olsoni* and the early Miocene coracoids show a crescent-shaped facies articularis (1), whereas it is ovate in the extinct *Nothura parvula* and *Nothura* sp. (0).
71. – Coracoid, groove for origin of ligamentum acrocoracohumerale, confluence with facies articularis clavicularis (Fig. 9): separated (0); confluent (1). After Bertelli and Chiappe (2005: character 20). This character is not related to the presence of a tuberculum brachiale (character 69; e.g. also occurs in *Tinamotis* and *Nothoprocta cinerascens*), and was scored as not comparable for all ratites included here because these taxa lack a facies articularis clavicularis. The early Miocene remains of MACN-SC-10 share with the extinct species of *Eudromia* (*Eudromia* sp. and *Eudromia olsoni*) a confluence of groove for ligamentum acrocoracohumerale and facies articularis clavicularis (1); whereas this condition is absent in the fossil species of *Nothura* (*Nothura* sp. and *Nothura parvula*) and MACN-SC-13.
72. – Coracoid, distinctly protruding processus acrocoracoideus (cranial projection relative to the facies articularis humeralis) (Fig. 9): present (0); absent (1). After Bertelli and Chiappe (2005: character 21). The coracoid lacks a cranially projected processus acrocoracoideus in *Crypturellus*, *Eudromia*, and *Tinamotis*. Bertelli and Chiappe (2005: characters 23 and 25) discussed the development and medial expansion of the processus acrocoracoideus within Tinamidae; however, we discarded these characters in view of its possibly continuous nature. After further study, we also found that the presence of a distinctive scar on the ventral surface of processus acrocoracoideus (Bertelli and Chiappe, 2005: character 22) is often indistinguishable or highly variable, and thus it was excluded from the analysis. *Eudromia olsoni*, and the oldest tinamous MACN-SC-10 and MACN-SC-13 lack a protruding processus acrocoracoideus (1), as opposed to other fossil tinamous (*Nothura parvula, Nothura* sp., and *Eudromia* sp.), where this process is well projected cranially (0).
73. – Coracoid, proximal margin of cotyla scapularis with pneumatic openings (Fig. 9): absent or few small foramina (0); perforated with large foramina (1). After Bertelli and Chiappe (2005, character 24). Pneumatization of this area is present in the living *Crypturellus*, *Eudromia*, *Tinamotis*, and the extinct taxa *Eudromia olsoni*, *Nothura* sp., MACN-SC-10, and MACN-SC-13.
74. – Coracoid, facies articularis scapularis (Fig. 9): shallow (0), excavated and cuplike (1). See Bertelli *et al*. (2011: character 37). As in extant Galliformes, the cotyla scapularis is shallow in all fossil and extant Tinamidae.
75. – Coracoid, base of processus procoracoideus, medial edge, distinctly projected crest (Fig. 9): absent (0); present (1). Bertelli and Chiappe (2005: character 26) discriminated three states of the crest development in tinamous; however, we considered the projection of this crest as a continuous character, only being able to corroborate the variation in the presence and absence in our sample. This crest is clearly delimitated in most tinamous (with the exception of *Tinamus* and *Nothocercus*) and the fossil taxa *Eudromia* sp., *Nothura* sp., and *Nothura parvula*.
76. + Coracoid, processus lateralis, dorsal view (Fig. 9): poorly developed or absent (0); developed, shorter or similar than sternal facet (1); well developed, distinctly longer than sternal facet, three-pointed sternal end (2). Bertelli and Chiappe (2005: character 28) distinguished the relative development of this process relative to the caudal width of the sternal facet to accommodate the greater variation seen in Tinamidae; only

Nothocercus lacks a distinct projected processus lateralis. Clarke (2004) described the presence of a developed lateral process in *Ichthyornis*. Although damaged, enough of the sternal end area is preserved to show that *Eudromia* sp. and *Nothura parvula* have a developed processus lateralis, and therefore were coded as (1/2).

77. + Coracoid, dorsal surface of distal end, impression for the m. sternocoracoidei: not pneumatized (0); only few openings developed (1); strongly pneumatized (2). Bertelli and Chiappe (2005, character 29) recognized only two conditions for this character that described the presence of pneumatic openings on the dorsal surface of the coracoid of some tinamous (e.g. most species of *Nothura* and *Nothoprocta*). We have added an additional state for this character to account for the strong pneumatization in the out-group taxa. These pneumatic openings are clearly absent in most extinct tinamous (with the exception of *Nothura parvula*).
78. – Humerus, ulna, radius, and carpometacarpus: well-developed separate elements (0); reduced or vestigial (1). These elements are reduced or vestigial in the out-group taxa *Apteryx* and *Rhea*.
79. – Humerus, incisura capitis obstructed by a tubercle projecting from the border of humeral head (Ericson, 1997: character 54; Fig. 9): absent (0); present (1). Livezey (1997: character 203) described the presence of a similar tubercle as the insertion of m. scapulohumeralis cranialis in some gruiforms. The presence in the forest tinamou *Crypturellus* of an incisura capitis enclosed by a distal projection of caput humeri was described by Bertelli and Chiappe (2005: character 30). This condition is also present in Galliformes. Because of its highly apomorphic morphology (character 77), the humerus of ratites cannot be coded for this character (and the following characters 79–81). *Eudromia olsoni* and *Nothura parvula* lack this tubercle on the caudal surface of the humerus.
80. + Humerus, crista bicipitalis, aspect in caudal view (Fig. 9): rounded, continuously curving (0); intermediate between squared off and rounded (1); distinctly squared off (generally with a hook-shaped extension) (2). Bertelli and Chiappe (2005: character 31) observed some variation in the degree of development among the specimens possessing a hook-shaped extension; however, after further examination of a more extensive sample, we do not consider this to be justification for an additional character state. Because the state assignment requires the presence of a crista bicipitalis, ratites were scored as non-comparable. Both *Eudromia olsoni* and *Nothura parvula* exibit a markedly squared off crista bicipitalis (2).
81. – Humerus, pneumatic foramina at bottom of fossa pneumotricipitalis (or corresponding area in taxa without such fossa) (Fig. 9): absent (0), present (1) (Mayr, 2011: character 77). Within tinamous (including the extinct taxa *Nothura parvula* and *Eudromia olsoni*), this opening is only absent in *Taoniscus*.
82. – Humerus, foramen pneumaticum surrounded by osseous ring or muscular scar (Fig. 9): no (0); yes (1). After Bertelli and Chiappe (2005: character 33). *Nothura*, *Nothoprocta*, and *Rhynchotus* show a distinct muscular mark bordering the fossa pneumotricipitalis ventralis. We consider this character non-comparable for taxa lacking a pneumatic fossa. In caudal view, the foramen pneumaticum is bounded by a muscular scar in *Nothura parvula* (1); *Eudromia olsoni* lacks this condition (0).
83. – Humerus, ventral condyle, length of main axis relative to that of dorsal condyle, cranial aspect (Fig. 9): shorter or subequal (0); longer (1). Our scorings differ from Bertelli and Chiappe (2005, character 36); we corroborated that all but one tinamou genera (*Tinamotis*) show a shorter ventral condyle (relative to the dorsal counterpart). This character (state 1) occurs in most Tinamidae and is also present in *Nothura parvula* and the early Miocene MACN-SC-H (1).
84. – Humerus, shallow and crescent-like impression for insertion of musculus brachialis (Fig. 9): no (0); yes (1). A sharply delimited impression brachialis occurs in most out-group taxa (with the exception of *Ichthyornis*). Because of its highly apomorphic morphology, the humerus of *Apteryx* and *Rhea* cannot be coded for this character. In *Nothura parvula* and MACN-SC-H the impression of musculus brachialis is a clearly flat scar (1).
85. – Humerus, processus supracondylaris dorsalis developed as a rounded and compact tubercle (Fig. 9): absent (0); present (1). A blunt process on the dorsal border of the distal humerus is found in most out-group taxa (with the exception of *Ichthyornis*). *Nothura parvula* and MACN-SC-H show a rounded and well-projected processus supracondylaris dorsalis (1).
86. – Humerus, processus supracondylaris ventralis (attachment of musculus pronator brevis of Howard, 1929), position (Fig. 9): on ventral surface or cranioventral margin (0); more cranially located (1). *Nothura parvula* and MACN-SC-H were coded as 0.
87. – Humerus, processus flexorius, distal prolongation viewed cranioventrallly (Fig. 9): absent (0); projects beyond the ventral condyle (1). This process does not project beyond the ventral

condyle in *Nothura parvula* and MACN-SC-H (0).

88. – Ulna/humerus proportions: about the same length (0); ulna distinctly longer than humerus (1); ulna shorter than humerus (2). Mayr (2011: character 82). The ulna only exceeds the humerus in length in *Tinamus*, *Tinamotis*, and *Eudromia* among tinamous, and is only shorter in *Taoniscus*. The ulna of *Tinamotis pentlandii* is distinctly longer than that of *Tinamotis ingoufi*. Preserved ulnae and humeri show similar proportions in *Nothura parvula* (0).
89. – Radius, distal end, expansion in ventral view (Fig. 9): distal end with curved aspect, one side more projected than the other (0); distal end wide, both sides expanded (1). The distal end of the radius of *Tinamotis* is typically expanded. *Nothura parvula* lacks this distal expansion (0).
90. – Carpometacarpus, fossa on ventral surface of proximal end, caudal to pisciform process (Fig. 9): absent or shallow (0); very deep (1). Bertelli and Chiappe (2005: character 43). This fossa is tentatively identified as the attachment for the ligamentum ulnocarpometacarpale ventralis (Baumel, 1993), and is extremely deep in most tinamous (including the fossil *Nothura parvula*) except for *Nothocercus*, where it varies from being virtually absent to deep. Because of its highly apomorphic morphology, the carpometacarpus of ratites cannot be coded for this character (and following character 86).
91. – Carpometacarpus, trochlea carpalis (Fig. 9): caudal rim of ventral portion with deep notch, shallow fossa infratrochlearis (0); caudal rim of ventral portion weakly notched or notch absent, deep and well-defined infratrochlear pit (1). The caudal rim of the ventral portion is clearly rounded with a distinct infratrochlear pit (tentatively identified as the attachment for the lig. radiocarpometacarpale ventralis; Baumel, 1993) in *Nothura*, *Taoniscus*, *Nothoprocta*, and the extinct taxa *Nothura parvula* (state 1).
92. + Ilium, dorsal surface, relative length of cranial and caudal portions, separated by the crista dorsolateralis ilii in dorsal view (Fig. 10), and by the acetabular area in lateral view (Fig. 10): cranial portion shorter than caudal portion (0); portions approximately of similar length or subequal (1); praeacetabular region distinctly longer than caudal portion, but less than twice the length of the latter (2); praeacetabular region around twice or more than twice the length of the postacetabular portion (3). Bertelli and Chiappe (2005: character 44) discriminated three states of relative length of praeacetabular and postacetabular iliac portions that we were able to corroborate in our sample (states 1, 2, and 3). A third condition, praeacetabular portion shorter (0), is typical of the out-group taxa.
93. – Pelvis, shape of the crista iliaca dorsalis at the acetabular area, dorsal view (Fig. 10): straight line or only slightly curved (0); markedly curved (1). The crista iliaca dorsalis is slightly curved in *Eudromia* and *Tinamotis*, but not as distinctly concave as in *Rhynchotus*, *Nothoprocta*, *Nothura*, and *Taoniscus* (condition 1), and thus the character was scored as 0. We scored *Rhea* and *Apteryx* as not comparable for this character.
94. – Pelvis, ala praeacetabularis ilii, cranial end rounded and markedly expanded laterally (Fig. 10): absent (0); present (1). The pelvis of the open-area tinamous (except for *Tinamotis* and *Eudromia*) and *Nothocercus* share a characteristic lateral projection of the ala praeacetabularis ilii.
95. + Pelvis, ilium, and ischium (Fig. 10): broadly fused, small fenestra present (0); fused over only a short distance, large fenestra present (1); not fused, fenestra open (2). Cracraft (1974: p. 503) considered the presence of a large, or open, fenestra a synapomorphy of ratites (see also Mayr 2011: character 94).
96. – Pelvis, ventral surface of postacetabular ilium (Fig. 10): ilioischiatic membrane attaches to ventrolateral edge of ilium (0); ridge for attachment of ilioischiatic membrane inset medially from lateral edge of ilium (1). fig. 12 in Houde (1988) described the development of a ventral ridge for the attachment of the ilioischiadic membrane in *Lithornis*. This lamina is also present in the Tinamidae (Bertelli, 2002).
97. – Ilium pars postacetabularis, caudal end markedly extended with 'tail'-like aspect (Fig. 10): absent or poorly developed (0); present (1). This character was considered not comparable for most out-group taxa (except *Lithornis*), which exhibit a broadly fused ilium and ischium. The caudal end of the ventral surface of the postacetabular ilium together with the synsacrum projects caudally in some open-area tinamous such as *Rhynchotus*, *Nothoprocta*, *Nothura*, and *Taoniscus*. In *Eudromia*, only a small flange is markedly less projected, and the taxon was thus scored as 0.
98. – Pelvis, maximum width (measurement at level of the acetabular area related to the cranial end of the praeacetabular area in dorsal view; Fig. 10): slightly wider (0); or nearly twice as wide as the praeacetabular width (1). The pelvis of *Tinamotis* is distinctly wider than the pelvis in other tinamous.
99. + Pubis, tuberculum praeacetabulare: absent or poorly developed, length shorter than acetabulum size (0); developed, approximately the same

size or slightly larger than the acetabulum (1); well projected, distinctly larger than acetabulum (2) (Mayr, 2011: character 93; Fig. 10). We observed variation in the degree of development of the tuberculum praeacetabulare among the specimens, and considered three character states. A well-developed tuberculum is typical of the forest tinamous (state 1), whereas a distinctly elongate process is present in the open-area genera (state 2). A third condition, praeacetabular portion shorter (0), is typical of the out-group taxa. This tubercle is small in *Lithornis* (Houde, 1988: fig. 21).

100. + Femur, development of the crista trochanteris (Fig. 11): little or no cranial projection (0); somewhat projected, but curved and medially directed, shallow fossa trochanteris (1); projects markedly, deep fossa (2). The variation of the degree of projection of the crista trochanteris fits into two different conditions within Tinamidae (states 1 and 2), the fossil *Nothura parvula* show a moderately projected crista trochanteris. A third condition, slight cranial projection (0), is typical of the out-group taxa.
101. + Femur/tarsometatarsus proportions: tarsometatarsus significantly longer than femur (0); about the same length as the femur (1); shorter than the femur (2); significantly shorter than the femur, does not reach the articular area distally (3). Worthy and Holdaway (2002: character 64) noted that the tarsometatarsus is longer than the femur in *Rhea*. We distinguish four states in this character. The tarsometatarsus of *Ichthyornis* is incompletely known. Although the only femur of *Nothura parvula* available to us was incomplete, the length of the preserved portion of this species indicates that the tarsometatarsus is comparatively much shorter than the femur (3).
102. – Femur, condylus medialis, articular surface in medial view (Fig. 11): proximal terminus of cranial rim much farther proximal than proximal terminus of caudal rim (0); proximal terminus of cranial rim subequal to proximal terminus of caudal rim (1). We distinguished two alternative conditions for the shape of the condylus medialis in medial view. The presence of a flattened surface is the most widely distributed condition within the taxa examined; only *Tinamotis*, *Eudromia*, and the extinct *Eudromia olsoni* show a sharply concave condylus medialis (state 1). *Nothura parvula* lacks this condition.
103. – Femur, markedly bowed (Fig. 11): absent (0); present (1). Among tinamous, *Nothoprocta* and *Rhynchotus* exhibit a strongly curved shaft; it is comparatively straight in other tinamou groups. This condition is absent in *Nothura parvula*.
104. – Tibiotarsus, condylus lateralis and medialis, relative length (Fig. 11): condylus lateralis distinctly longer (0); condylus lateralis subequal or slightly longer than medialis (1). Our scoring differs from Bertelli and Chiappe (2005: character 53); we consider a subequal condylus lateralis the same condition as the slightly longer than condylus medialis. The forest tinamous exhibit an elongated condylus lateralis (state 0), which, unlike the open-area groups, is relatively longer than the tarsometatarsus. Variation in the relative width of the condylus lateralis and medialis for tinamous was also described by Bertelli and Chiappe (2005: character 51); however, after further study of a more extensive sample, we found no substantial differences among species of Tinamidae. Condition 1 is present in the fossil *Nothura parvula* and MACN-SC-T. We consider the highly derived morphology of the condyles of *Rhea* to be non-comparable for this character.
105. – Tibiotarsus, crista cnemialis cranialis (Fig. 11): distinctly longer in the proximodistal direction than crista cnemialis lateralis (0); short, similar distal projection relative to the crista cnemialis lateralis (1). The crista cnemialis cranialis of most tinamous (and out-groups) is relatively longer than the crista cnemialis lateralis (state 0); the alternative condition (state 1) occurs only in *Eudromia*, *Tinamotis* (Bertelli and Chiappe, 2005: character 48), and the extinct *Eudromia olsoni*; *Nothura parvula* lacks this condition.
106. – Tibiotarsus, sulcus extensorius, distinct medial location (Fig. 11): absent (0); present (1) (Ericson, 1997: character 44). In tinamous (including the fossil taxa *Nothura parvula* and MACN-SC-T), ratites, and *Lithornis*, the groove that houses the tendon for the extensor muscles of the digits is displaced towards the medial margin of the bone (Parker, 1866; Pycraft, 1900). This condition is different from the condition seen in most neognaths, where the groove is normally located towards the centre of the shaft.
107. – Tibiotarsus, pons supratendineus (Fig. 11): absent (0), present (1) (Mayr 2011: character 100). This feature was coded as present in *Apteryx* by Mayr (2011) and Lee *et al*. (1997), but absent in *Apteryx* by Bledsoe (1988). As Cracraft (1974: 500) discussed, the supratendinal bridge occasionally does not ossify completely in *Apteryx*, and so is coded as variable in this analysis. A pons supratendineus is present in Tinamidae and also preserved in the extinct *Nothura parvula* and MACN-SC-T.
108. – Tibiotarsus, condylus lateralis, shape in cranial view (Fig. 11): proximal margin angular, widens distally (0); elongated with rounded proximal end

(1); short with a more rounded aspect (2). Our scorings differ from Bertelli and Chiappe (2005: character 52); we consider the highly derived condyle morphology of *Rhea* to be non-comparable for this character. In most tinamous (including the fossil taxa *Nothura parvula* and MACN-SC-T), the shape of the condylus lateralis remains elongated along its entire length when viewed in cranial aspect, with a rounded proximal end (state 1). This condition differs from that present in *Tinamus*, where the condyle is more pointed and widens distally, being somewhat triangular in shape (state 0), and also differs from *Tinamotis*, which has a short and rounded condyle (state 2).

109. – Tarsometatarsus, hypotarsus, general shape, and distal extension of hypotarsal ridges relative to foramina vascularia proximalia (Fig. 12): truncated and squared off, ending approximately at level of or proximal to foramina (0); acuminated, ending markedly distal to foramina (1). After Bertelli and Chiappe (2005: character 63). *Nothocercus* and *Tinamus major* share the presence of a distally truncated hypotarsus with several out-group taxa (e.g. Galliformes, among others); the alternative condition (state 1) is present in other extant tinamous and the fossil *Nothura parvula*.
110. – Tarsometatarsus, hypotarsus (Fig. 12): with several well-developed cristae intermediae (0); one well-developed, proximally prominent crista (and a low ridge, if present) (1). Because the positional homology of these ridges is uncertain, we code only the number of prominent ridges. *Nothura parvula* shows a hypotarsus with a developed crista (1).
111. + Tarsometatarsus, hypotarsus, hypotarsal sulcus/canal for m. flexor digitorum longus, proximal view (Fig. 12): developed as a broad, plantary open sulcus, without medially bordering cristae (0); developed as a broad, plantarly open sulcus that is separated by distinct cristae (1); nearly enclosed canal (2); fully enclosed canal (3). The degree of aperture of the sulcus/canal for m. flexor digitorum longus varies within Tinamidae, from a nearly closed canal in the forest groups (state 2) to a broader, plantary open sulcus in the open-area groups (states 0 and 1); the latter group shares this condition with *Rhea*, *Apteryx*, and *Lithornis*. *Nothura parvula* shares with extant open-area tinamous the presence of a broad sulcus (1).
112. – Tarsometatarsus, hypotarsus, sharp medial ridge at cotyla medialis (Fig. 12): present (0); absent (1) (Bledsoe, 1988: character 69). This ridge is present in most Tinamidae (including the fossil taxa *Nothura parvula*) and *Lithornis* (Houde 1988: 23); it is only absent in *Eudromia*.
113. – Tarsometatarsus, fossa parahypotarsalis lateralis (Fig. 12): shallow (0); marked and deeply excavated (1). *Nothura parvula* lacks a deep fossa parahypotarsalis lateralis (0).
114. – Tarsometatarsus, foramen vasculare distale (Fig. 12): well developed (0); vestigial, almost completely closed (1). The foramen is only reduced in *Tinamotis*, among the sample examined. This condition is absent in *Nothura parvula*.
115. + Tarsometatarsus, distal trochleae, relative distal extension of trochleae metatarsorum II and IV (Fig. 12): trochlea metatarsi II more distally projected than trochlea metatarsi IV (0); both trochleae about equally projected distally, distal ends of incisurae intertrochleares lateralis medialis et lateralis leveled (1); trochlea metatarsi II slightly less distally projected than trochlea metatarsi IV, but reaching distally beyond as proximal margin of incisura interterochlearis lateralis (2); trochlea metatarsi II much less distally projected than trochlea metatarsi IV, without reaching proximal margin of incisura interterochlearis lateralis (3). Within Tinamidae, the distal end of trochlea metatarsi II is at approximately the same level as that of trochlea metatarsi IV only in *Tinamotis* (state 1), and it is comparable to that of *Apteryx*; by contrast, the trochlea metatarsi II is shorter (state 2) in *Eudromia*, *Taoniscus*, and *Nothura* (including the fossil *Nothura parvula*), or is distinctly less projected than trochlea metatarsi IV in the forest tinamous and *Rhynchotus* and *Nothoprocta* (state 3).
116. + Hallux, development (Mayr 2011: character 110 modified): absent (0); greatly reduced, measuring less than half of the length of the proximal phalanx of third toe) (1); long (2). A hallux is completely reduced only in *Eudromia* and *Tinamotis*, whereas in all other tinamous it is present but short (state 1). Although the hallux is not preserved, it is possible to score its presence in *Nothura parvula* (12), as the fossa metatarsi I is clearly developed on the distal end of the tarsometatarsus.
117. – Ligamentum orbitoquadratum (Elzanowski, 1987): absent (0); present (1). According to Elzanowski (1987; fig. 50A–D), this ligament tying the processus orbitalis of the quadrate to the braincase only occurs in tinamous.
118. – Ligamentum postorbitale, origin: frontal part of the processus postorbitalis (0); pleurosphenoid part of the process (1); ossiculum postorbitalis (covers the frontal and pleurosphenoid parts of the process) (2). In tinamous (and most ratites, except for *Apteryx*), the insertion of this ligament occurs in the jugal bar and is probably related to the movement of the upper mandible (Elzanowski, 1987).

119. – Ligamentum jugomandibulare internum: absent (0); present (1). This typical ligament of the avian head is absent in tinamous (Elzanowski, 1987).
120. – Ligamentum jugomandibulare externum, insertion: undivided (0); bipartite (1). Only in *Crypturellus* does this ligament bifurcate at the end, and thus the insertion at the supraangular area of the mandible is clearly bipartite (Elzanowski, 1987). The ligamentum jugomandibulare externum is present in all birds except for Galliformes and Anhimidae (Dzerzhinskii, 1983), therefore these taxa were coded as non-comparable for this character.
121. – Ligamentum quadratomandibulare rostrale: absent (0); present (1). This ligament (from the body of the quadrate to the mandible) is well developed in most tinamous except for *Nothoprocta* and *Tinamotis* (Elzanowski, 1987).
122. + Ligamentum quadratomandibulare rostrale: extensive, not divided (0); bipartite, with medial and lateral parts (1); only medial part present (2). Both medial and lateral parts of this ligament are developed in *Crypturellus*. Only the medial part of this ligament is present in *Tinamus*, and the lateral part is present in *Nothura* and *Eudromia*; an extensive ligament that occupies the position of both parts (lateral and medial) occurs in *Rhynchotus* (Elzanowski, 1987). Because of the absence of this structure, the condition for *Nothoprocta* and *Tinamotis* was coded as non-comparable.
123. – Ligamentum sphenomandibulare: absent (0); present (1). This tendinous band that connects the mandible with the lamina parasphenoidalis is found, among tinamous, only in *Tinamus* and *Eudromia* (Elzanowski, 1987).
124. + Aponeurosis parabasalis, attachment: to postmeatic area (0); to both the postmeatic area and lamina basitemporalis (1); to lamina basitemporalis (2). According to Webb (1957) the aponeurosis parabasalis is present in *Rhea* among the out-group taxa, with attachment on the postmeatic area of the ala tympanica caudalis, on the occipital surface of the skull. Among tinamous, a postmeatic attachment was also described for *Crypturellus* and *Tinamus* (Elzanowski, 1987). Unlike these taxa, the attachment is exclusively (or at least mainly) to the basal plate (lamina basitemporalis) in *Eudromia*, *Tinamotis*, *Rhynchotus*, and *Nothoprocta*; an intermediate state is present in *Nothura* that combines both conditions equally (Elzanowski, 1987).
125. – Musculus adductor mandibulae externus, pars caudalis: absent (0); present (1). The m. adductor mandibulae externus of most birds is divided into four parts: superficialis, medialis, profunda, and caudalis. In most tinamous (except for *Tinamus* and *Crypturellus*), the pars caudalis is absent (Elzanowski, 1987).
126. – Musculus adductor mandibulae externus, origin on temporal fossa: absent (0); present (1). The cranial origin of this muscle is limited to the processus zygomaticus in most tinamous (and ratites), with the exception of *Eudromia* and *Tinamotis*, the area of origin of which extends onto the braincase (Elzanowski, 1987).
127. – Musculus adductor mandibulae externus, parajugal branch of pars profunda: absent (0); present (1). This branch is absent in *Nothura*, *Nothoprocta*, and *Rhynchotus* among tinamous (Elzanowski, 1987).
128. + Musculus adductor mandibulae externus, pars profunda, and superficialis: fused (0); partially separated (1); separated (2). In *Rhynchotus* and *Nothoprocta*, the m. adductor mandibulae externus is partially tripartite (with pars superficialis and pars profunda partially fused state 1); alternatively, it is bipartite (pars superficialis and profunda fused into pars rostralis, state 0) in *Eudromia*, *Tinamotis*, and *Nothura*, and tripartite (condition 2) in *Crypturellus* and *Tinamus* (Elzanowski, 1987).
129. – Musculus intramandibularis: absent (0); present (1). The m. intramandibularis is part of the pseudotemporalis complex, and it is only present in *Tinamus*, *Nothura*, *Rhynchotus*, and *Nothoprocta* (with the exception of *Nothoprocta cinerascens*) (Elzanowski, 1987).
130. – Musculus pseudotemporalis, ventral temporal portion: absent (0); present (1). The m. pseudotemporalis originates from the temporal fossa and inserts to the medial surface of the mandible (George and Berger, 1966). The subdivision of this muscle into three portions (two pars orbitales and one pars temporalis) is a generalized character in tinamous (and also in most ratites), in which the temporal fossa is almost entirely occupied by the m. pseudotemporalis (Elzanowski, 1987). In *Tinamus*, *Crypturellus*, and *Nothura*, the origin extends ventrally onto the pleuroesphenoid area (ventral head) (Elzanowski, 1987). The presence of a ventral head of pars temporalis was also described for several neognathous birds (Elzanowski, 1987).
131. – Musculus pseudotemporalis, attachment to os suprangulare: absent (0); present (1). In tinamous, the insertion of this muscle occurs on the tuberculum pseudotemporale of the mandible, near the processus medialis mandibularis; only in *Crypturellus* is it also attached to the os supraangulare (on the dorsal area of the tuberculum) (Elzanowski, 1987).

132. – Musculus pseudotemporalis and m. quadratomandibularis, complete or almost complete separation: absent (0); present (1). In most tinamous (except for *Eudromia* and *Tinamotis*), these muscles are connected both at the origin and insertion (Elzanowski, 1987).
133. – Musculus quadratomandibularis, insertion: beyond the dorsal margin of the mandible (0); does not extend so far dorsally (1). The m. quadratomandibularis attaches on the medial surface of the mandible of tinamous (fossa caudalis mandibulae), and extends beyond the dorsal margin of the mandible in *Rhynchotus*, *Eudromia*, *Tinamotis*, and *Nothoprocta* (state 0); the alternative condition (state 1) is present in *Tinamus*, *Nothura*, and *Crypturellus* (Elzanowski, 1987).
134. – Musculus quadratomandibularis, aspect at origin: thin, superficial aponeurosis (0); strong aponeurotic sheet (1). The origin of m. quadratomandibularis of tinamous from the processus orbitalis of the quadrate is weak, except in *Eudromia*, which exhibit a strong aponeurosis (Elzanowski, 1987).
135. – Musculus pterygoideus, pars medialis: separated into three unnipennate portions (0); complex multipennate system (1). This muscle (including the pseudotemporalis profundus and depressor mandibulae) participates in the movement (closing) of the mandible (Baumel, 1993). In tinamous, it is subdivided into pars medialis and lateralis (Elzanowski, 1987: fig. 53). The morphology of the pars medialis shows two different patterns in tinamous: *Tinamus*, *Crypturellus*, and *Nothura* have three well-separated unnipenate portions, whereas in *Rhynchotus*, *Nothoprocta*, *Tinamotis*, and *Eudromia* these portions are interconnected, forming a multipennate pars medialis (Elzanowski, 1987).
136. – Musculus pterygoideus, fasciculus caudalis: absent (0); present (1). Absent in *Nothura*, *Tinamus*, and *Crypturellus* (Elzanowski, 1987).
137. – Musculus pterygoideus, pars medialis enclosed in aponeurotic sheath: absent (0); present (1). In *Norhoprocta* and *Rhynchotus*, all dorsal and ventral aponeuroses are fused, enclosing pars medialis in a conspicuous aponeuroric sheath (Elzanowski, 1987).
138. – Musculus protractor pterygoidei et quadrati: undivided (0); bipartite (1). In most tinamous (except for *Tinamus* and *Crypturellus*), the m. protractor et quadrati consist of two parts: pars superficialis and pars profunda. No division of this muscle has been described for ratites (Elzanowski, 1987).
139. – Musculus depressor mandibulae externus, insertion: on fossa caudalis mandibularis (0); extending beyond fossa caudalis (1) (Elzanowski, 1987).
140. – Musculus columellae, perforated by n. glossopharyngealis et vagi: absent (0); present (1). Only in *Nothura* and *Nothoprocta* is this muscle peforated by the exit of the n. glossopharyngealis et vagi (Elzanowski, 1987).
141. – Musculus levator palpebrae dorsalis, muscular portion: well developed (0); poorly developed, thin layer (1). In *Nothura*, *Nothoprocta*, and *Rhynchotus*, this muscle consists of a well-developed proximal muscular part and an extensive fascial sheet (fascia supraocularis; Elzanowski, 1987). In other groups, the proximal part is much thinner and semitransparent.
142. – Musculus levator palpebrae dorsalis, origin from os ectethmoidale: absent (0); present (1). Only in *Eudromia* and *Tinamotis* is there a rostral attachment of the m. levator palpebrae dorsalis (Elzanowski, 1987).
143. – Musculus orbicularis palpebrarum, morphology: muscular fibres (0); ligament (1). A replacement of muscular fibres by elastic ligaments in m. orbicularis palpebrarum occurs in *Eudromia* and *Tinamotis* (Elzanowski, 1987).
144. – Musculus orbicularis palpebrarum, origin from ossicula supraorbitales: absent (0); present (1). *Crypturellus*, *Tinamus*, *Eudromia*, *Nothocercus*, and some species of *Nothoprocta* share the presence of the ossiculum supraorbitalis on the dorsal surface of the area interorbitalis; however, the origin of the m. orbicularis palpebrarum from these ossicles has been described only for *Crypturellus* (Elzanowski, 1987). This character has been coded as non-comparable for other tinamous (without ossiculum supraorbitalis).
145. – Musculus depressor palpebrae ventralis: well developed (0); vestigial (1). In *Tinamus* and *Crypturellus*, the m. depressor palpebrae ventralis is vestigial and fused to the m. tensor periorbitae. By contrast, in other tinamous both muscles are well developed (Elzanowski, 1987).
146. + Musculus obliquus dorsalis, origin: muscle undivided (0); divided into two parts (1); divided into three parts (2). The m. obliquus dorsalis shows at the origin three morphological patterns among tinamous. The condition present in *Nothura* and *Rhynchotus* is characterized by the division of the muscle into two parts, and three in *Nothoprocta*, whereas the origin is undivided in the other genera (Elzanowski, 1987).
147. – Musculus coracobrachialis cranialis, enormously developed: absent (0); present (1). This muscle originates on the processus acrocoracoideus of the coracoid and inserts on the cranial surface of the humerus. The large size of the m.

coracobrachialis cranialis is a distinct feature of tinamous, exceeding that found in any other group of birds (Hudson *et al*., 1972).

148. – Musculus deltoideus, pars minor, caput ventrale fused to m. supracoracoideus: absent (0); present (1). The caput ventrale of this muscle, which originates from the m. sternocoracoclavicularis and inserts on the crista deltopectoralis of the humerus (Baumel, 1993), is over most of its length completely fused to the m. supracoracoideus in tinamous, being separated only at the triosseal canal (Hudson *et al*., 1972).
149. – Musculus latissimus dorsi, pars caudalis, origin extensive: absent (0); present, attached to two ribs (1); very extensive, attached to four ribs (2). The large size of the pars caudalis of m. latissimus dorsi (= m. latissimus dorsi posterior of Hudson *et al*., 1972), with an extensive origin, is typical of tinamous and a few other groups (e.g. loons, auks, penguins; Hudson *et al*., 1972). Tinamous show two different conditions: in *Tinamus* and *Crypturellus*, the origin is very extensive, between the musculus serratus superficialis, pars metapatagialis and pars caudalis, including the second to fifth ribs, and the cranial area of the ilium. The alternative condition and the most generalized is a less extensive surface of origin, including only the fourth and fifth ribs and the cranial area of the ilium. This character was considered ordered.
150. – Musculus latissimus dorsi, pars metapatagialis, relative position to the m. serratus superficialis: over dorsal surface (0); adjacent (1). The pars metapatagialis of m. latissimus is very rare among birds (Baumel, 1993), and, if present, inserts into the humeral feather tract with pars metapatagialis of m. serratus superficialis. This uncommon muscle is present in tinamous, and lies adjacent to the m. serratus superficialis in *Crypturellus*, *Tinamus*, and *Eudromia*, whereas it passes over the dorsal surface of this muscle in other tinamous (Hudson *et al*., 1972).
151. – Musculus interosseus dorsalis, insertion: undivided (0); divided (1). This muscle, together with the m. interosseus ventralis, fills the intermetacarpal space (Baumel, 1993). A double tendon for insertion to phalanx II and III (origin from the dorsal surface of the carpometacarpus and metacarpals II and III), is a typical feature of tinamous (Hudson *et al*., 1972).
152. + Musculus ulnimetacarpalis dorsalis, origin: only dorsal head present (0); bipartite, small ventral head (1); bipartite, large ventral and dorsal head (2). The origin of this muscle on the distal end of the ulna of tinamous is divided into a large ventral and dorsal head in *Tinamus* and *Crypturellus*, the ventral head is poorly developed in other tinamous (and completly absent in *Tinamotis*). The m. ulnimetacarpalis dorsalis is vestigial in *Apteryx* (McGowan, 1982), and was coded as non-comparable for this character.
153. Musculus supinator, distinctly longer: absent (0); present (1). This muscle is much longer in *Tinamus* and *Crypturellus* (Hudson *et al*., 1972).
154. – Musculi iliotrochanterici cranialis and medius: separated (0); fused (1). The m. iliotrochanterici, related to protraction movements of the femur, originate on the praeacetabular ilium and insert on the trochanter femoris (Baumel, 1993). The m. iliotrochantericus cranialis (= iliotrochantericus iliacus or anterior of Hudson *et al*., 1972) and medius are present in Megapodiidae and most other birds (George and Berger, 1966). These muscles are also separated in most tinamous, except for *Tinamus* and *Crypturellus*, in which the m. iliotrochantericus cranialis is fused throughout the m. iliotrochantericus medialis (Hudson *et al*., 1972).
155. – Musculus fibularis longus, sesamoid: absent (0); present (1). Specimens of *Crypturellus soui*, *Crypturellus cinnamoneus*, and *Crypturellus boucardi* show a sesamoid enclosed in the tendon of the m. fibularis longus (= m. peronaeus longus of Hudson *et al*., 1972).
156. – Musculus flexor hallucis longus and m. flexor digitorum longus: not fused (0); fused (1). The tendons of these muscles (related to the flexion movements of hallux and digits II, III, and IV) are fused at the middle of the tarsometatarsus, except in *Nothura* and *Nothoprocta*. After fusion, branches go only to the three fore-toes in *Eudromia* and *Tinamotis*, which lack a hallux (Hudson *et al*., 1972). As this is related to the absence of a hallux (character 111), this condition, and other muscles associated with it (e.g. extensor hallucis longus, flexor hallucis brevis, etc.), was not coded for this analysis, to avoid redundant coding.

SUPPORTING INFORMATION

Additional supporting information may be found in the online version of this article at the publisher's web-site:

Appendix S1. Comparative material used in the construction of the data matrix. AMNH, American Museum of Natural History (New York, USA); BMNH, The Natural History Museum (London, UK); FML, Fundación Miguel Lillo (Tucumán, Argentina); FMNH, Field Museum (Chicago, USA); HA, Museu de História Natural de Taubaté (Sao Paulo, Brazil); KU, University of Kansas, Museum of Natural History (Lawrence, USA); LACM, Natural History Museum of Los Angeles County (Los Angeles, USA); LSUMZ, Louisiana State University, Museum of Natural Science, Louisiana State University (Baton Rouge, USA); MACN, Museo Argentino de Ciencias Naturales "Bernardino Rivadavia" (Buenos Aires, Argentina); MCZ, Museum of Comparative Zoology, Harvard University (Cambridge, USA); MLP, Museo La Plata (La Plata, Argentina); MVZ, University of California, Museum of Vertebrate Zoology (Berkeley, USA); SMF, Forschungsinstitut und Natur-Museum Senckenberg (Frankfurt, Germany); UMMZ, Museum of Zoology (Ann Arbor, USA); USNM, National Museum of Natural History (Washington D.C., USA); YPM, Yale Peabody Museum of Natural History (New Haven, USA); ZMUC, Zoological Museum University of Copenhagen.